Collective laser cooling of two trapped ions

A. W. Vogt,* J. I. Cirac,† and P. Zoller
Joint Institute for Laboratory Astrophysics, University of Colorado
and National Institute of Standards and Technology, Boulder, Colorado 80309-0440
and Institut für Theoretische Physik, Universität Innsbruck, Technikerstrasse 25, A-6020 Innsbruck, Austria
(Received 3 March 1995)

Collective laser cooling of two ions moving in a trapping potential is studied theoretically in the limit when the distance between the ions is smaller or comparable to the wavelength of the exciting laser light. A set of rate equations for the population of the trap levels is derived in the Lamb-Dicke limit, and for low laser intensities describing the effects of dipole-dipole interaction and super- and subradiance on the cooling dynamics.

PACS number(s): 32.80.Pj

I. INTRODUCTION

Many-body and collective atomic phenomena are presently of central interest in the investigation of trapped and laser cooled atoms [1]. In the context of ion traps, recent experiments have reported the storage of a few tens of ions in linear and ring traps, as well as the formation of ion crystals [2–5] (see [6] for a recent review). The purpose of this paper is to study theoretically *collective* effects in laser cooling in the simple system of two ions moving in a trapping potential [7]. (For two unbound atoms, see [8].) We are particularly interested in a situation in which the two ions are close together at a distance comparable to or smaller than the wavelength of the exciting laser light. This research is motivated in part by recent progress in building microtraps [9,10], which have an extremely strong confining potential for the ions and thus force the ions to small distances [11].

Collective effects in laser cooling of trapped ions manifest themselves both in the external and internal dynamics. First, the Coulomb interaction couples the motion of the ions in the trap. Thus the ions perform oscillations corresponding to the collective eigenmodes of the ions around their equilibrium positions, resulting from the Coulomb repulsion and the trapping force. Second, for distances comparable to the wavelength of the light, the internal structure of the two ions forms a ''quasimolecule,'' where the dipole-dipole interaction couples and splits the unperturbed atomic levels. In addition this interaction modifies the atomic spontaneous decay rate, leading to the formation of a superradiant and a subradiant (metastable) manifold with a radiative decay constant that is larger or smaller than the unperturbed single-atom decay width, respectively [12].

Many-particle laser cooling is one of the most active subjects in atom physics. With recent developments and the appearance of new techniques, very low temperatures at high densities have been achieved during the last few years [13]. One of the goals of this branch of physics is to observe quantum statistical effects related to the bosonic or fermionic nature of the atomic sample [1]. At the conditions required to observe these phenomena, atom-atom interactions become important. In fact, it has been predicted and observed that with the usual laser cooling techniques dipole-dipole interactions lead to extra heating forces at sufficiently high densities [14,15]. For neutral atoms the interplay between cold atomic collisions and laser cooling is an extremely complex theoretical problem [16]. In contrast to the case of neutral atoms, laser cooling of two interacting ions in a trap provides a theoretically tractable but nonetheless experimentally realizable model system, which can provide important insights on our way to understanding more complex many-body systems. From the theoretical point of view, the two-ion system has the advantage that ions at sufficiently low temperatures perform only small oscillations around their equilibrium positions. This allows an expansion in terms of a small parameter, which corresponds basically to the ratio of the amplitude of the oscillations to the wavelength of the laser exciting an internal transition (Lamb-Dicke limit [17]). The cooling of vibrational modes of trapped-ion clusters has already been studied by Javanainen [18]. For the case of two ions, we go beyond that analysis by including dipole-dipole interaction. This interaction is reflected in the cooling rates and final temperatures. Thus, from the experimental point of view, two trapped ions constitute a unique system in which basic dipole-dipole interactions and super- or subradiant effects [19,20] can be studied in detail without the complications due to short-range interactions in atomic collisions and quantum statistical effects.

The paper is organized as follows. In Sec. II, a qualitative overview and some of the basic results are given, stressing the differences in comparison with the single-atom case. In Secs. III and IV, they are derived in more detail. In Sec. V we give a deeper analysis of the results. Finally, Sec. VI contains a summary of the main results.

II. OVERVIEW

The purpose of this section is to give a qualitative overview and summary of the essential physics of laser excitation and cooling of two ions in a trap. We are particularly interested in the case in which the two ions are at a distance

*Present address: Institut für Theoretische Physik, Bunsenstrassa 9, D-37073 Göttingen, Germany.
†Permanent address: Departamento de Fisica, Universidad de Castilla-La Mancha, 13071 Ciudad Real, Spain.

smaller than the laser wavelength λ so that dipole-dipole interaction between the ions and modification of the ion lifetime (superradiance) are important. For comparison with the two-ion case we start with a brief review of laser cooling of a *single* trapped ion [17]. A detailed derivation of our results for two ions, based on a master-equation treatment, will be presented in the following sections.

A. Single-ion laser cooling

Let us consider an ion with ground and excited states $|g\rangle$, $|e\rangle$ (possibly degenerate); transition frequency ω_0; and spontaneous decay rate 2γ. The ion moves in a harmonic trap centered at $\mathbf{x}=0$, with frequencies $\nu_{x,y,z}$ along the three principal axes. We will denote the corresponding oscillator states by $|\mathbf{n}\rangle=|n_x,n_y,n_z\rangle$, with quantum numbers $n_u=0,1,\ldots$ $(u=x,y,z)$. The ion is excited by a laser beam of frequency ω_L, which induces transitions between ground and excited levels, and also changes the motional state. In the low-intensity limit (below saturation), the atom spends most of its time in its ground state $|g\rangle$. In this case it is simple to derive rate equations that describe the change of the motional state after an absorption or spontaneous-emission cycle . They are given by [21,17]:

$$\frac{d}{dt}\pi_{\mathbf{m}}=\sum_{\mathbf{n}\neq\mathbf{m}}(\Gamma_{\mathbf{m}\leftarrow\mathbf{n}}\pi_{\mathbf{n}}-\Gamma_{\mathbf{n}\leftarrow\mathbf{m}}\pi_{\mathbf{m}}), \tag{1}$$

where $\pi_{\mathbf{n}}=\langle\mathbf{n}|\langle g|\rho|g\rangle|\mathbf{n}\rangle$ is the population of level $|\mathbf{n}\rangle$, and the transition rates from level $|\mathbf{n}\rangle$ to $|\mathbf{m}\rangle$ are

$$\Gamma_{\mathbf{m}\leftarrow\mathbf{n}}=2\gamma\frac{3}{8\pi}\sum_{\lambda=1,2}\int d\Omega_{\hat{\mathbf{k}}}\left|\langle\mathbf{m}|\langle g|e^{-i\mathbf{k}\cdot\mathbf{x}}[\boldsymbol{\epsilon}^{\lambda}(\hat{\mathbf{k}})\cdot\mathbf{D}^{\dagger}]\frac{1}{H_{\mathrm{eff}}-E_{\mathbf{n}}}H_L(\mathbf{x})|g\rangle|\mathbf{n}\rangle\right|^2. \tag{2}$$

In this equation, H_L is the Hamiltonian describing the atom-laser interaction, and H_{eff} is the free effective (non-Hermitian) Hamiltonian for the free evolution of the ion in the trap, including the decay of the excited-state population due to spontaneous emission. The energy of the state $|\mathbf{n}\rangle|g\rangle$ is $E_{\mathbf{n}}$, i.e., $H_{\mathrm{eff}}|\mathbf{n}\rangle|g\rangle=E_{\mathbf{n}}|\mathbf{n}\rangle|g\rangle$. The position operator is denoted by $\mathbf{x}$, and $\mathbf{D}$ is the dipole operator for the transition from the ground to the excited levels. Finally, $\mathbf{k}$ and $\boldsymbol{\epsilon}^{\lambda}$ are the wave vector and a unit vector corresponding to polarization λ of each spontaneously emitted photon, respectively. The interpretation of the transition amplitude is simple if one reads it from right to left: the ion initially in its ground internal state and in the oscillator state $|\mathbf{n}\rangle$ is excited by absorbing laser light, and after free evolution it returns to the ground state by emitting a spontaneous photon. The rates are summed (integrated) over the possible polarizations (directions) of the spontaneously emitted photon. Given the dependence on the position operator of $e^{-i\mathbf{k}\cdot\mathbf{x}}$ and H_L, the oscillator state changes to the state $|\mathbf{m}\rangle$ because of the recoil in the absorption and emission processes.

In current experiments with single ions, the motion of the trapped atom is restricted to a region of space that is small compared to the laser wavelength, so that the Lamb-Dicke limit holds [17]. In this case, formula (2) can be further simplified by expansion of $e^{-i\mathbf{k}\cdot\mathbf{x}}$ and H_L around $\mathbf{x}=0$, including terms up to first order,

$$\Gamma_{\mathbf{m}\leftarrow\mathbf{n}}=2\gamma\frac{3}{8\pi}\sum_{\lambda=1,2}\int d\Omega_{\hat{\mathbf{k}}}|\boldsymbol{\epsilon}^{\lambda}(\hat{\mathbf{k}})\cdot[\mathbf{b}-i\mathbf{d}(\hat{\mathbf{k}})]|^2, \tag{3}$$

where

$$\mathbf{b}\equiv\langle\mathbf{m}|\langle g|\mathbf{D}^{\dagger}\frac{1}{H_{\mathrm{eff}}-E_{\mathbf{n}}}H_{\mathrm{L}}^{(1)}|g\rangle|\mathbf{n}\rangle, \tag{4a}$$

$$\mathbf{d}(\hat{\mathbf{k}})\equiv\langle\mathbf{m}|\langle g|\mathbf{D}^{\dagger}(\mathbf{k}\cdot\mathbf{x})\frac{1}{H_{\mathrm{eff}}-E_{\mathbf{n}}}H_{\mathrm{L}}^{(0)}|g\rangle|\mathbf{n}\rangle. \tag{4b}$$

Here $H_L^{(0)}$ ($H_L^{(1)}$) denotes the zeroth- (first-) order expansion of the atom-laser interaction Hamiltonian (for a detailed definition see the following section). In the Lamb-Dicke limit the quantum oscillator state can change only by ±1. For example, considering how the motion can change along the direction $p=x,y,z$, there are two kinds of rates: the rate $\Gamma_{n_p+1\leftarrow n_p}$ describes heating processes, while $\Gamma_{n_p-1\leftarrow n_p}$ corresponds to cooling. In particular, **b** and **d** are directly related to the amplitudes corresponding to the following two processes [17]:

(i) The trap state is changed during the excitation by the laser ($|g;n_p\rangle\rightarrow|e;n_p\pm1\rangle$) and remains unchanged in the subsequent spontaneous emission ($|e;n_p\pm1\rangle\rightarrow|g;n_p\pm1\rangle$). This corresponds to a heating-cooling process.

(ii) The laser excites the atom without affecting the trap state ($|g;n_p\rangle\rightarrow|e;n_p\rangle$), which is changed in a subsequent spontaneous emission ($|e;n_p\rangle\rightarrow|g;n_p\pm1\rangle$) of a photon with direction $\hat{\mathbf{k}}$ and polarization $\boldsymbol{\epsilon}^{\lambda}(\hat{\mathbf{k}})$. This is a diffusion process.

Since the two different amplitudes in Eq. (3) are added, there is, in principle, interference between these two channels. However, the cross term of the square is an odd function of the integration variable $\hat{\mathbf{k}}$, and therefore it vanishes upon doing the integration over $d\Omega_{\hat{\mathbf{k}}}$. That is, when averaging over all possible spontaneous emission processes, the interference disappears.

On the other hand, since the matrix elements $\langle n_p\pm1|\mathbf{x}|n_p\rangle$ and $\langle n_p\pm1|H_L^{(1)}|n_p\rangle$ contain factors $\sqrt{n_p+1}$ or $\sqrt{n_p}$, the rates have the form $\Gamma_{n_p+1\leftarrow n_p}=(n_p+1)A_{p+}$, $\Gamma_{n_p-1\leftarrow n_p}=n_pA_{p-}$. The coefficients $A_{p\pm}$ completely determine the dynamics and the steady state of the ion in the trap [17]. In particular, cooling takes place along the p direction if $A_{p-}>A_{p+}$. This occurs for red (negative) laser detunings $\Delta\equiv\omega_{\mathrm{L}}-\omega_0$, since in that case the laser absorption process in which the ion decreases the oscillator quantum number is closer to resonance than the one increasing it. It is then easy

to see that there are two regimes in laser cooling of a trapped ion: (i) for $\gamma > \nu_p$ we are in the regime of Doppler cooling where the final energy of the ion is of the order of $\hbar\gamma$; (ii) for $\gamma < \nu_p$ the two motional sidebands at $-\Delta \pm \nu_p = 0$ are well resolved (sideband cooling limit), and the ions can be cooled to the vibrational ground state. In either case the steady state is a thermal distribution (Bose-Einstein distribution) [17,22] with an average phonon number of

$$\langle n_p \rangle = \frac{A_{p+}}{A_{p-} - A_{p+}}. \tag{5}$$

B. Two ions in a trap: Basic concepts

1. Equilibrium position

We consider now two ions of mass m and charge e confined in a trap. The trapping potential is again assumed to be harmonic and the (single-ion) oscillation frequencies along the x, y, and z axes are denoted by $\nu_{x,y,z}$, respectively. We define center-of-mass and relative coordinates as follows:

$$\mathbf{R}' \equiv \frac{1}{\sqrt{2}}(\mathbf{x}^{(1)} + \mathbf{x}^{(2)}), \quad \mathbf{r}' \equiv \frac{1}{\sqrt{2}}(\mathbf{x}^{(1)} - \mathbf{x}^{(2)}). \tag{6}$$

The equilibrium position for the center-of-mass coordinates will be at $\mathbf{R}' = 0$, and for the relative coordinate it is determined by balancing the Coulomb potential with the trapping force; i.e., it is given by the minimum of

$$U(\mathbf{r}') = \frac{m}{2}\sum_i \nu_i^2 r_i'^2 + \frac{\beta}{|\mathbf{r}'|} \tag{7}$$

with $\beta = e^2/4\pi\epsilon_0\sqrt{2}$. For $\nu_z < \nu_x$, ν_y the minimum of $U(\mathbf{r}')$ will be located on the z axis at $\mathbf{r}_0' = r_0'\hat{e}_z$, with $r_0' = (\beta/m\nu_z^2)^{1/3}$. Thus, the classical equilibrium positions for the two ions are obtained from $\mathbf{R}' = \mathbf{0}$, $\mathbf{r}' = \mathbf{r}_0'$ as

$$\mathbf{X}^{(1,2)} = \frac{1}{\sqrt{2}}(0 \pm \mathbf{r}_0') = \pm\frac{r_0'}{\sqrt{2}}\hat{e}_z, \tag{8}$$

with equilibrium distance $|\mathbf{X}^{(1)} - \mathbf{X}^{(2)}| = \sqrt{2}r_0' \equiv r_0$.

2. Spectroscopy of the two-ion system for fixed positions

We consider now a situation in which the ions are fixed at their equilibrium positions. For the internal structure we assume a (dipole-allowed) angular momentum $j_g = 0 \rightarrow j_e = 1$ transition. This is motivated by our interest in the role of the laser polarization in laser cooling, and this is the simplest model to display these effects. The atomic states of the two ions $\alpha = 1,2$ are labeled by $|g, m=0\rangle_\alpha$ and $|e, m=0,\pm1\rangle_\alpha$, with m Zeeman quantum numbers. For the internal quantum states of the two ions we will adopt the notation $|a;b\rangle \equiv |a\rangle_1 |b\rangle_2$. For a large distance such that $a \equiv kr_0 \gg 1$ (with $k = \omega_0/c$), the two ions essentially do not interact. With decreasing a the degeneracy of the (bare) states, where one of the ions is in the ground state, and the other ion is in the excited state, is lifted by the dipole-dipole interaction. The dipole-dipole coupling also modifies the spontaneous lifetime of the ions [23]. For reasons that will become clear in the context of Fig. 6(b) below we discuss this interaction employing the excited-state basis $\{|e_u\rangle, u = x,y,z,\}$, defined in terms of angular momentum eigenstates as $|e_z\rangle = |e, m=0\rangle$, $|e_x\rangle = (|e,m=-1\rangle - |e,m=1\rangle)/\sqrt{2}$, and $|e_y\rangle = i(|e,m=-1\rangle + |e,m=1\rangle)/\sqrt{2}$. Thus the eigenenergies and eigenstates of this two-ion system, in a frame rotating at the laser frequency, are

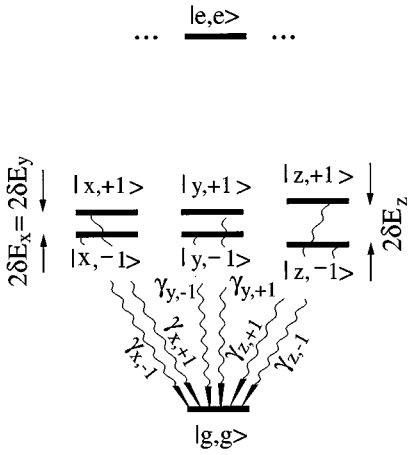

FIG. 1. Level structure for two two-level atoms ($0 \rightarrow 1$ transition). "$\ldots |e;e\rangle \ldots$" represents the nine doubly excited states.

$$E_{g;g} = 0 \quad |g;g\rangle,$$

$$E_{u,\pm1} = -\hbar\Delta \pm \delta E_u - i\hbar\gamma_{u,\pm1} \quad \text{for } |u,\pm\rangle \equiv (|e_u;g\rangle \pm |g;e_u\rangle)/\sqrt{2}, \tag{9}$$

$$E_{e_i;e_u} = -2\hbar\Delta - i2\hbar\gamma \quad |e_i;e_u\rangle$$

[see Eq. (34) below]. Here 2γ is the decay rate of each atom, $\Delta = \omega_L - \omega_0$ is the detuning, and the level shifts δE_u and widths $\gamma_{u,\pm1}$ are given in Sec. III [see Eq. (34) below].

In Fig. 1 we have plotted this level configuration for the two-ion system. The level shifts and decays of the intermediate levels are indicated on the figure, too. We note that in the limit of small distances, $a \rightarrow 0$, the $|u,-1\rangle$ states become metastable while the spontaneous emission rate of the state $|u,+1\rangle$ doubles. This is related to the well-known collective effect of sub- and superradiance [23]. A graph of the shift $\delta E_u/(2\hbar\gamma)$ and decay rate $2\gamma_{u,\pm1}/(2\gamma)$ as a function of the scaled distance $a = kr_0$ is shown in Fig. 2. In this figure we have marked by a vertical dotted line the point corresponding to $a = 2\pi/8$, which we have chosen as the "standard" distance for most of our plots below. We have chosen this relatively small distance in order to make the collective effects clearly visible.

We consider now laser excitation with linear polarization in the direction $u = x$, y, or z. Thus, the laser can couple the ground state $|g;g\rangle$ only to the excited two-ion states $|u,\pm1\rangle$ given in Eq. (9). The corresponding coupling strengths also depend on the propagation direction of the laser, as well as on the interatomic distance. For example, when the laser propagates along the x axis, only the states $|x,+1\rangle$ can be excited (for processes without phonon interactions). This is due to the fact that both ions see the same

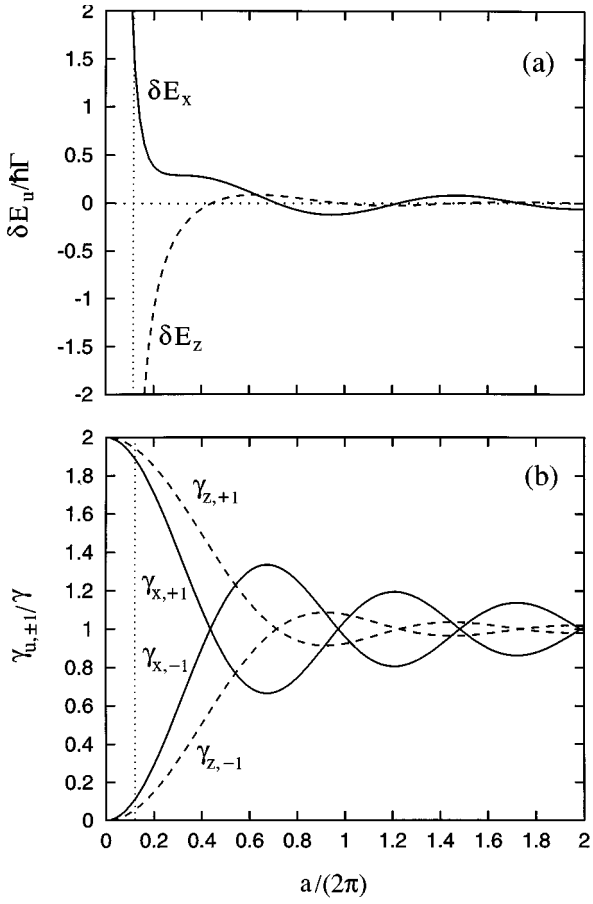

FIG. 2. Level shifts $\delta E_{x,z}$ (a) and modified linewidths $\gamma_{u,\pm 1}$ (b) for the singly excited states $|x,\pm 1\rangle$ and $|z,\pm 1\rangle$ as a function of the scaled distance $a=kr_0$. $\Gamma\equiv 2\gamma$.

laser phase, and therefore the state excited must be symmetric under interchange of the label indices of the ions. On the other hand, for a propagation direction along the z axis, the relative phase seen by the ions depends on their separation $a=kr_0$, which enters the coupling matrix element from the ground to the excited state.

3. Small oscillations around the equilibrium positions

The center-of-mass motion is governed by a harmonic potential with unperturbed trap frequencies $\nu_{x,y,z}$. When the oscillation amplitudes of the ions around their equilibrium positions are small, one can use a linearized analysis for the relative motion coordinates. In this case, the eigenfrequencies are $\nu_{rx,ry}=\sqrt{\nu_{x,y}^2-\nu_z^2}$, $\nu_{rz}=\sqrt{3}\nu_z$ where the first two frequencies correspond to a shearing motion perpendicular to the ion axis $\mathbf{r}_0'$, and the third frequency is associated with an oscillation along the z axis. These eigenoscillations of the center-of-mass and relative motion are readily quantized. We will denote the corresponding oscillator states by $|n_x n_y n_z;n_{rx}n_{ry}n_{rz}\rangle$ with quantum numbers $n_u, n_{ru}=0,1,2,\ldots$ $(u=x,y,z)$.

A necessary condition for the linearization in the relative motion to be valid is the smallness of the parameter

$$\zeta_u=\sqrt{\frac{\hbar}{2m\nu_{ru}}}\Big/ r_0\equiv\eta_{ru}/a\ll 1, \tag{10}$$

which is the ratio of the ground-state width of the u component to the equilibrium distance of the ions as given by the Coulomb repulsion. By virtue of $e^2/4\pi\epsilon_0=\alpha\hbar c$, where α is the fine-structure constant, $\alpha\approx 1/137$, the equilibrium distance can be expressed as $\mathbf{r}_0=(2\alpha\hbar c/m\nu_z^2)^{1/3}$ and therefore

$$\zeta_u=(\hbar\nu_z/\alpha^2 mc^2)^{1/6}2^{-1}(\nu_z/\nu_{ru})^{1/2}. \tag{11}$$

Thus, as long as the trap frequency can be considered small compared to optical frequencies, the parameters ζ_u are small. Therefore one can safely use the linearized analysis to describe the motion in terms of harmonic oscillators for both center-of-mass and relative coordinates [24]. Our model also neglects the micromotion: this assumes that the (collective) ion oscillation frequencies are much smaller than the applied external rf driving frequencies. In the present model calculation, this is consistent with the lowest-order Lamb-Dicke expansion for the laser-ion and dipole-dipole interaction (see Ref. [25] for a discussion of the micromotion on laser cooling).

C. Two ions in a trap: Laser cooling

In order to study the cooling in the system of two ions, we proceed in a similar way as that for a single trapped ion. We first find the rate equations in the low-intensity limit. Second, we expand the transition rates in the Lamb-Dicke limit, and identify the physical processes that are involved in these transitions. By including the dipole-dipole interaction, we will go beyond the analysis presented previously by Javanainen [18].

1. Low-intensity limit

In the low-intensity limit, the trap populations evolve much slower than the coherences between trap states or the internal degrees of freedom, which therefore can be adiabatically eliminated. This leads in second-order perturbation theory to the rate equations (1), where now $\pi_{\mathbf{n}}=\langle\mathbf{n}|\langle g;g|\rho|g;g\rangle|\mathbf{n}\rangle$ is the population of level $|g;g\rangle|\mathbf{n}\rangle$, and the rates are given by

$$\Gamma_{\mathbf{m}\leftarrow\mathbf{n}}=2\gamma\frac{3}{8\pi}\sum_{\lambda=1,2}\int d\Omega_{\hat{\mathbf{k}}}\left|\langle\mathbf{m}|\langle g;g|\sum_{\alpha=1,2}e^{-i\mathbf{k}\cdot\mathbf{x}^{(\alpha)}}[\boldsymbol{\epsilon}^{\lambda}(\hat{\mathbf{k}})\cdot\mathbf{D}^{(\alpha)\dagger}]\frac{1}{H_{\mathrm{eff}}(\mathbf{x}^{(1)}-\mathbf{x}^{(2)})-E_{\mathbf{n}}}H_L(\mathbf{x}^{(1)},\mathbf{x}^{(2)})|g;g\rangle|\mathbf{n}\rangle\right|^2. \tag{12}$$

The form of this equation is similar to that of Eq. (2), but now we are summing over contributions from both atoms, in which the superscript $\alpha=1,2$ specifies the first and second ion, respectively. Furthermore, now the free effective Hamiltonian $H_{\rm eff}$ includes the dipole-dipole interactions, which depend explicitly on the position operator for the relative motion. We note that the motional state can now also change because of dipole-dipole interaction.

2. Lamb-Dicke limit

Similar to the single-ion case, we assume that the oscillation amplitudes of the center-of-mass and relative motion around their equilibrium values are much smaller than the laser wavelength; i.e., the Lamb-Dicke parameters (proportional to the ratio of the ground-state width of the oscillators to the optical wavelength) are small:

$$\eta_{u,ru}=k\sqrt{\frac{\hbar}{2m\nu_{u,ru}}}\ll 1, \quad (u=x,y,z). \tag{13}$$

In this paper we are interested in the case in which the ions are closer than a wavelength, since it is there that two-particle effects become important. This regime requires large trap frequencies, and therefore the Lamb-Dicke limit is valid. Then we can expand the rates (12) in terms of the η's. To second order in the Lamb-Dicke parameters, the transition rate (12) from state $\mathbf{n}$ to state $\mathbf{m}$ is

$$\Gamma_{\mathbf{m}\leftarrow\mathbf{n}}=2\gamma\frac{3}{8\pi}\sum_{\lambda=1,2}\int d\Omega_{\hat{\mathbf{k}}}|\boldsymbol{\epsilon}^{\lambda}(\hat{\mathbf{k}})\cdot[\mathbf{b}+\mathbf{c}-i\mathbf{d}(\hat{\mathbf{k}})]|^2, \tag{14}$$

where

$$(\mathbf{b},\mathbf{c},\mathbf{d})=\sum_{\alpha=1,2}e^{-i\mathbf{k}\cdot\mathbf{X}^{(\alpha)}}(\mathbf{b}^{(\alpha)},\mathbf{c}^{(\alpha)},\mathbf{d}^{(\alpha)}), \tag{15}$$

and we have defined

$$\mathbf{b}^{(\alpha)}\equiv\langle\mathbf{m}|\langle g;g|\mathbf{D}^{(\alpha)\dagger}\frac{1}{H_{\rm eff}^{(0)}-E_{\mathbf{n}}}H_{\rm L}^{(1)}|g;g\rangle|\mathbf{n}\rangle, \tag{16a}$$

$$\mathbf{c}^{(\alpha)}\equiv\langle\mathbf{m}|\langle g;g|\mathbf{D}^{(\alpha)\dagger}\frac{1}{H_{\rm eff}^{(0)}-E_{\mathbf{n}}}(-H_{12}^{(1)})\frac{1}{H_{\rm eff}^{(0)}-E_{\mathbf{n}}}\times H_{\rm L}^{(0)}|g;g\rangle|\mathbf{n}\rangle, \tag{16b}$$

$$\mathbf{d}^{(\alpha)}(\hat{\mathbf{k}})\equiv\langle\mathbf{m}|\langle g;g|\mathbf{D}^{(\alpha)\dagger}[\mathbf{k}\cdot(\mathbf{x}^{(\alpha)}-\mathbf{X}^{(\alpha)})]\frac{1}{H_{\rm eff}^{(0)}-E_{\mathbf{n}}}H_{\rm L}^{(0)}\times|g;g\rangle|\mathbf{n}\rangle, \tag{16c}$$

with $H_{12}^{(1)}$ the first-order expansion of the dipole-dipole interaction. The rates are different from zero only if $\mathbf{m}$ differs from $\mathbf{n}$ by ±1 in exactly one out of the six vibrational modes: $|\mathbf{m}\rangle\equiv|n_x\pm1\,n_yn_z;n_{rx}n_{ry}n_{rz}\rangle$, etc. In the following we will use the notation $|\mathbf{m}\rangle\equiv|\ldots n_p\pm1\ldots\rangle$, where the index $p=x,y,z,rx,ry,rz$. With this notation the formulas look very similar to those of the single-ion case. In particular, for $|\mathbf{m}\rangle\equiv|\ldots n_p+1\ldots\rangle$ the transition rate has the form $\Gamma_{\mathbf{m}\leftarrow\mathbf{n}}=(n_p+1)A_{p+}$, where A_{p+} is a constant independent of n_p. Similarly, $\Gamma_{\mathbf{m}\leftarrow\mathbf{n}}=n_pA_{p-}$ if $|\mathbf{m}\rangle\equiv|\ldots n_p-1\ldots\rangle$. Cooling occurs in mode p if $A_{p-}>A_{p+}$, and the resulting distribution is again thermal, with an average phonon number given in Eq. (5).

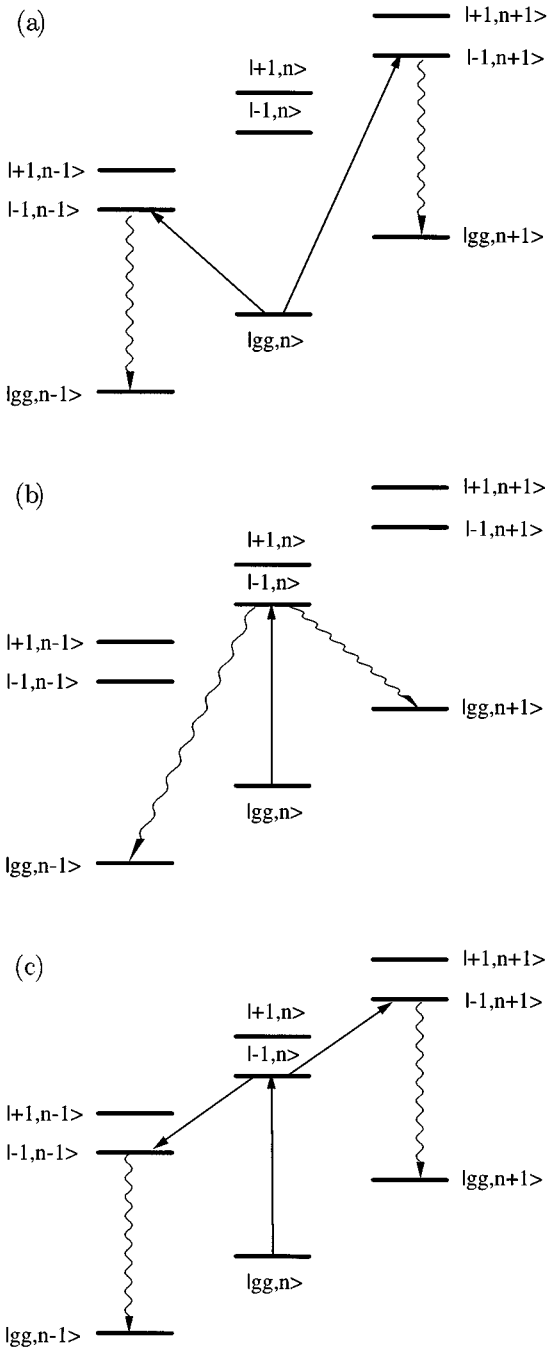

FIG. 3. Processes in second-order perturbation theory for phonon creation or annihilation by laser excitation of some state $|\cdot,-1\rangle$; similarly via $|\cdot,+1\rangle$.

The physical interpretation of these terms can be read off as in the single-ion case. Now, there are three contributions:

(i) Vectors $\mathbf{b}$ describe processes in which the atom-laser interaction takes the system from the ground level to an excited state and changes the number of quanta in the oscillator p. A spontaneous emission leads back to the ground state without changing the oscillator states [Fig. 3(a)]. This is analogous to the process described by $\mathbf{b}$ in the single-ion

case, which led to cooling for negative detunings from resonance.

(ii) Vectors **d** refer to the atom-laser interaction taking the system from the ground to an excited level without changing the oscillator states. A subsequent spontaneous emission leads back to the ground state and changes the number of quanta in the oscillator state p [Fig. 3(b)]. As in the single-atom case, this is a diffusion process giving equal contributions to A_{p+} and A_{p-}.

(iii) Vectors **c** stand for processes in which the atom-laser interaction takes the system from the ground to an excited level without changing the oscillator states. The dipole-dipole interaction changes the number of quanta in the oscillator states p and possibly couples to a different excited state. A spontaneous emission leads back to the ground state without changing the vibrational quantum numbers [Fig. 3(c)]. There is no analogue for this in the single-atom case. It can therefore be expected that this process leads to novel physical effects when compared to laser cooling of a single ion.

It is worth mentioning that process (iii) does not contribute to the modification of the center-of-mass motion since it is due to the dipole-dipole interaction, which depends on the relative position of the ions. On the other hand, for the relative motion it can have important consequences in the cooling process. In particular, it gives rise to the possibility of having transverse cooling, i.e., cooling of the y and z components by a laser propagating in the x direction. Apart from that, the corresponding amplitude of this process can interfere with the other processes leading to the enhancement or the decrease of the cooling rate. This depends on whether the interference is constructive or destructive. These kinds of phenomena are entirely due to two-atom interactions, and therefore they have no analogue in the single-ion case, where there are no interference effects in the Lamb-Dicke limit. In the following we briefly summarize the most relevant results in terms of the coefficients $A_{p\pm}$, which, as mentioned above, completely determine the properties of the cooling process. Note that to reach the regime in which the atoms are closer than an optical wavelength, one needs very strong trap frequencies. In this case, not only is the Lamb-Dicke limit fulfilled but also we are typically in the strong confinement limit, where the trap frequencies are larger than the spontaneous decay rate. Thus, in this regime we expect to find, among other phenomena, sideband cooling for negative detunings close to the trap frequency of the corresponding mode.

D. Two ions in a trap: Results and discussion

The results for laser cooling of two ions in a trap depend on several parameters. On the one hand, there are six modes of motion (center-of-mass and relative motion) that display different (cooling) dynamics. Depending on the specific geometry of the problem (the directions of laser propagation and polarization), only part of these modes are excited by the atom-laser interaction. On the other hand, given a specific polarization of the laser—for example, linear along the direction u—only the internal excited sublevels $|e;u\rangle$ can be excited. Finally, laser cooling depends on the specific parameters, such as the laser detuning Δ, the trap frequencies $\nu_{x,y,z}$, spontaneous decay rate 2γ, and the distance between the equilibrium positions of the ions (which is characterized by the parameter a).

Given the numerous possibilities for the geometry of the atom-laser interaction, we will discuss here a few cases that display the basic phenomena in the problem. A more detailed discussion is given in Sec. V. As mentioned above, there are mainly two differences between laser cooling of two ions with respect to the single-ion case: (i) in the case of two ions the dipole-dipole interaction leads to level shifts and changes the decay rates; (ii) the dipole-dipole interaction is responsible for a physical process that changes the motion of the ions. In this respect, the center-of-mass modes have a different behavior than the relative motion modes, since (ii) applies only to the latter. Here we will first describe cooling of the center-of-mass modes, and then we will analyze the more complicated case of the relative modes.

1. Center-of-mass motion

Let us concentrate on the situation in which the laser propagates along the z axis with linear polarization along the x axis. We first consider the case in which the ions are far apart from each other ($a=kr_0>1$). Under these circumstances, the shifts and rates due to dipole-dipole interaction are very small, and therefore the ions behave independently [18]. Laser cooling is then almost identical to the single-ion case. In Fig. 4(a) we have plotted the coefficient $A_{z\pm}$ (solid and dashed lines, respectively) for the z component of the center-of-mass mode as a function of the laser detuning. Here, we have taken a laser propagating in the z direction with polarization along the x axis. As in the single-ion case, for red (negative) detunings $A_{z-}>A_{z+}$ (i.e., there is cooling), whereas for blue (positive) detunings there is heating. Maximum cooling rates occur at $\Delta=-\nu_z$, which corresponds to the sideband cooling regime, whereby each time that one of the ions absorbs a laser photon its motional quantum state decreases by 1. The width of the resonances appearing in the figure are of the order of γ since they are related to the spontaneous-emission process. Obviously, the motion along the other two directions x,y is not cooled by the laser (only heated because of the diffusion accompanying each spontaneous emission).

When the ions are closer together ($a=kr_0<1$) superradiant effects are reflected in the cooling process. For example, in Fig. 4(b) we have plotted $A_{z\pm}$ (solid and dashed lines, respectively) for a scaled ion separation $a=2\pi/8$. Now, each of the peaks has split into a doublet, separated by $2\delta E_x/\hbar$ [compare Eq. (9)]. The narrow peaks correspond to excitation of the state $|x,-1\rangle$ whereas the broad ones belong to the superradiant state $|x,+1\rangle$. Thus, the widths of the peaks are given by $\gamma_{x\pm1}$, respectively. Laser cooling occurs for negative detunings (close to the lower motional sideband), and it is maximum at $\Delta\pm\delta E_x/\hbar=-\nu_z$. (Remember that $\Delta=\omega_L-\omega_0$ denotes the detuning of the laser with respect to the unperturbed atomic frequency. Hence, the detunings with respect to the levels $|x,\pm1\rangle$ are $\Delta\mp\delta E_x/\hbar$ etc. Since the level shifts $\delta E_u/\hbar$ are small compared to the trap frequencies in our examples, the lower sideband resonances $\Delta\mp\delta E_x/\hbar=-\nu_z$ still occur at $\Delta\approx-\nu_z$.) Cooling can be understood as before since the lower sideband excitations of

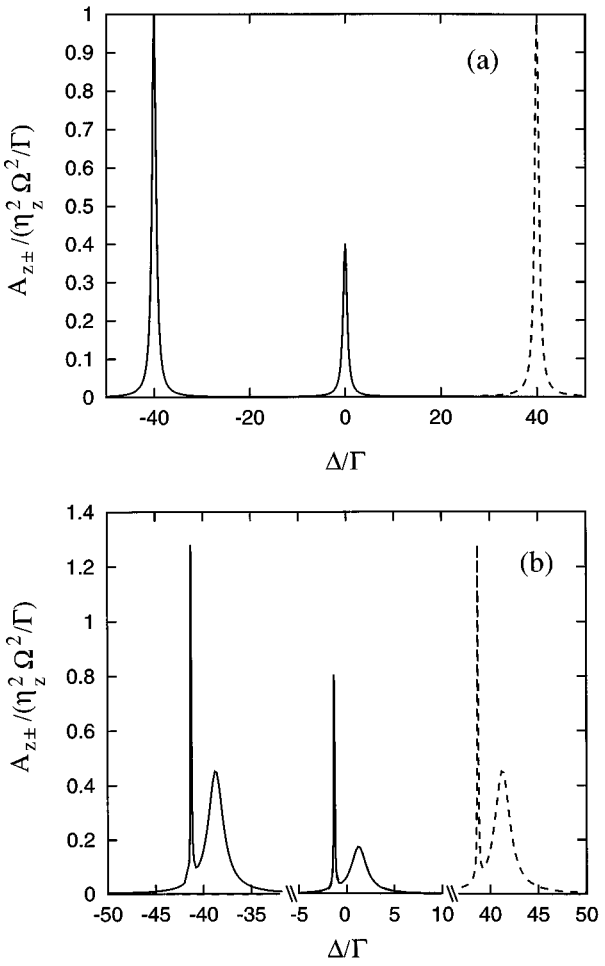

FIG. 4. Cooling and heating coefficients A_{z-} (solid curve) and A_{z+} (dashed curve) for the z component of center-of-mass motion of two ions. Laser configuration $\mathbf{V}(\mathbf{x})=\hat{\mathbf{e}}_x e^{ikz}\Omega/2$. (a) Large equilibrium distance: $a=20\pi$; (b) small distance: $a=2\pi/8$. At the central peaks the dotted and dashed lines overlap. $\Gamma\equiv 2\gamma$.

the sub- and superradiant states do not interfere; cf. Sec. V C. As mentioned before, for the center-of-mass motion only the vectors **b** [process of Fig. 3(a)] and **d** [process of Fig. 3(b)] contribute to the ion dynamics. The process of Fig. 3(a) leads to sideband cooling whenever the laser frequency is close to one of the two lower sideband resonances (in the figure, those that couple to the states $|x\pm 1;n-1\rangle$). The process of Fig. 3(b) leads to diffusion. On the other hand, in contrast to the single-ion case, the heights of the peaks (i.e., the amplitudes of these processes) depend on the particular geometry of the laser excitation. Since each of the vectors **b** and **d** is the sum of two other vectors related to the spontaneous emission in each individual ion, the amplitudes depend on the relative phase between these terms. This is the basis for sub- and superradiant behavior [cf. Eqs. (A4), (A5), and (A8) in Appendix A].

2. Relative motion

We concentrate now on a discussion of the relative motion of the ions. The interesting case is again when the ions are close, $a=kr_0<1$. Now the resonances appear around detunings $\Delta\simeq 0,\pm\nu_{rx,ry,rz}$. In addition to the phenomena discussed in the case of the center-of-mass modes, there is an extra process that takes place [Fig. 3(c)], which is due to the position dependence of the dipole-dipole interaction. Here we will concentrate on the physical consequences of this process.

We assume that the laser propagates along the y axis, linearly polarized along the x direction. Because of the polarization, laser excitation couples the ground state $|g;g\rangle$ only to the states $|x,\pm 1\rangle$. Furthermore, for the processes in which the motional quantum numbers do not change in the excitation step, and for this configuration, the laser light couples the ground state $|g;g\rangle$ only to the state $|x,+1\rangle$, since for this configuration the laser phase seen by both ions is the same and therefore the excited state must be symmetric under interchange of the labels that number the ions. For processes in which the excitation is accompanied by the creation or annihilation of a phonon of relative motion, the reverse holds: for them, only the state $|x,-1\rangle$ can be excited with the present laser configuration.

In Fig. 5 we have plotted the coefficients $A_{rx\pm}$ [Fig. 5(a)], $A_{rz\pm}$ [Fig. 5(b)], and $A_{ry\pm}$ [Fig. 5(c)] as a function of the detuning for $a=2\pi/8$. First note that even if the laser is propagating along the y direction, the x and z components of the relative motion coordinate can be cooled for negative detunings. At first sight, this is quite surprising since the photons absorbed by the ions (which are the ones that can be controlled—through an appropriate detuning—in the single-ion case) can only change the motion along the y component. In other words, for the rx and rz components only the diagrams of Figs. 3(b) and 3(c) contribute (i.e., the vector **b** is identically zero). Thus, the physical reason of this transverse cooling is not related to the momentum transfer in the ion-laser interaction. It is rather due to the dipole-dipole interaction since this interaction does not explicitly depend on the direction of the laser propagation. Thus, it is the diagram of Fig. 3(c) that is responsible for this effect, i.e., the vector **c** in the rate given in Eq. (12). Note that cooling of the ry direction is dominated by sideband cooling since in that case $\mathbf{b}\neq 0$.

For close to zero detunings [see Figs. 5(a) and 5(b)], the mode rx is heated ($A_{rx,+}>A_{rx-}$), whereas the mode rz is cooled ($A_{rz,+}>A_{rz-}$). Let us analyze in more detail the excitation processes mediated by dipole-dipole interaction [Fig. 3(c)]. In the first stage, the system of ions is excited by laser absorption to the state $|x,+1;\mathbf{n}\rangle$ starting from $|g;g;\mathbf{n}\rangle$. In the next step, the oscillator state is changed because of the dipole-dipole interaction. Depending on which relative motion mode is changed (rx or rz) the corresponding transition is $|x,+1;n_{rx}\rangle\rightarrow|z,+1;n_{rx}\pm 1\rangle$ [Fig. 6(b)] or $|x,+1;n_{rz}\rangle\rightarrow|x,+1;n_{rz}\pm 1\rangle$ [Fig. 6(a)], respectively. That is, the dipole-dipole interaction may change the atomic polarization when inducing transitions that change the motional state. Spontaneous emission takes the atoms back to the ground internal states without changing the vibrational quantum numbers. Thus, the change of the quantum number n_{rx} is accompanied by a change of polarization. This in turn is responsible for the different behavior in the rx and rz components. Aside from all that, now the amplitudes **c** and **d** can interfere, even after integrating over spontaneously emitted photons. This interference leads to modifications in the central peak, depending on the relative phase of these two am-

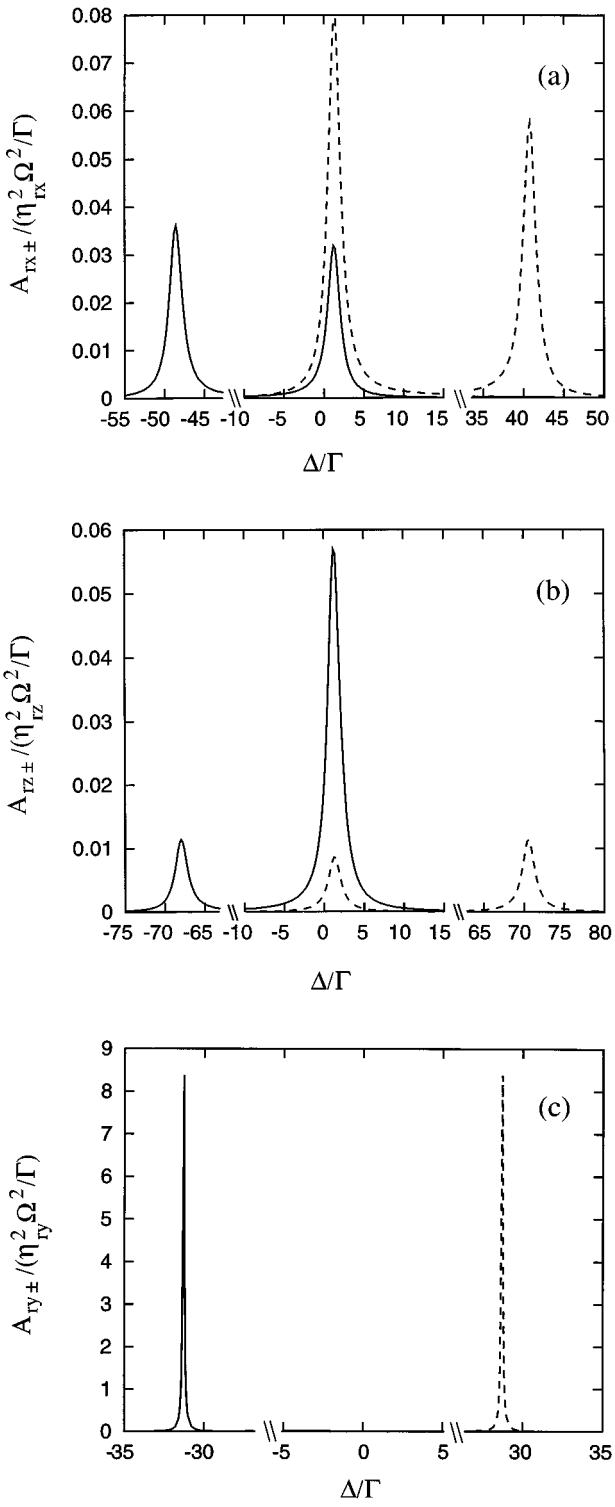

FIG. 5. Cooling and heating coefficients $A_{x,y,z-}$ (solid curve) and $A_{x,y,z+}$ (dashed curve) for the x, y, and z components of relative motion of two ions. Laser configuration $\mathbf{V}(\mathbf{x})=\hat{\mathbf{e}}_{\mathbf{x}}e^{iky}\Omega/2$. $\Gamma\equiv 2\gamma$.

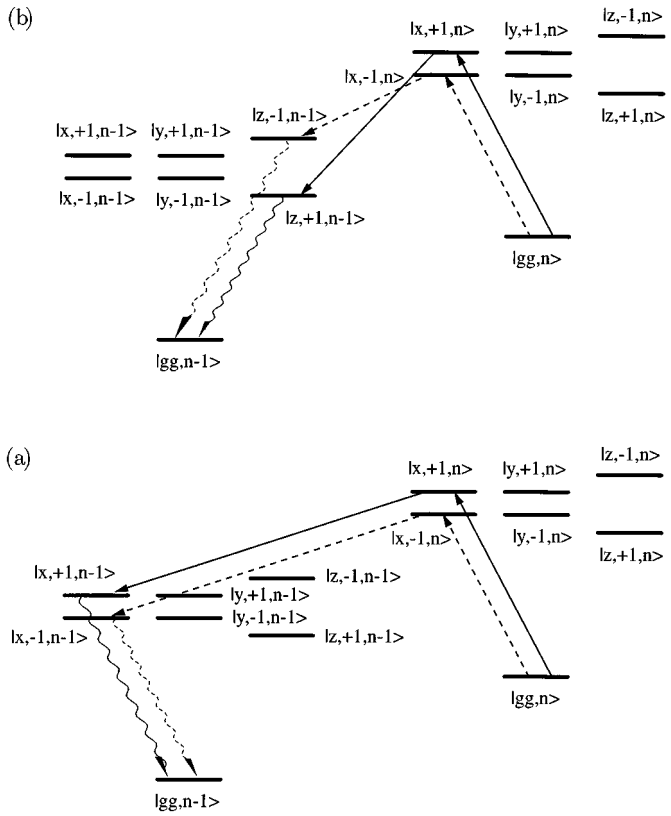

FIG. 6. Processes resulting from dipole-dipole interaction in the cooling of (a) z, and (b) x component of relative motion for laser light polarized in the x direction.

plitudes. These effects will be discussed in more detail in Sec. V. We will show there that the contribution of the dipole-dipole term **c** relative to the sideband cooling and diffusion amplitudes **b** and **d** is given by the dimensionless parameter $9\gamma/(\nu_p a^4)$, which for the parameters in our example is of the order of 15%.

Finally, Fig. 5(c) shows $A_{ry,\pm}$ as a function of the detuning. In this case, while the sideband cooling-heating amplitude $\mathbf{b}\neq 0$, we have the dipole-dipole term $\mathbf{c}=0$, so that this is similar to the single-ion case. Because of polarization selection rules, the only possible processes are $|g;g;n_{ry}\rangle\rightarrow|x,-1;n_{ry}\pm 1\rangle\rightarrow|g;g;n_{ry}\pm 1\rangle$ (which leads to sideband heating-cooling at $\Delta+\delta E_x/\hbar=\pm\nu_{ry}$) and $|g;g;n_{ry}\rangle\rightarrow|x,+1;n_{ry}\rangle\rightarrow|g;g;n_{ry}\pm 1\rangle$ (which leads to diffusion for $\Delta\simeq 0$). The central peak in Fig. 5(c) is so small as to be invisible on the chosen scale. This is due to a combination of the following factors: (i) the occurrence of a term $1/\gamma_{x,+1}^2$ at resonance, which is smaller than the $1/\gamma_{x,-1}^2$ term in the sideband resonances via the state $|x,-1\rangle$, and (ii) the fact that in processes with creation or destruction of a phonon of *relative* motion, the decay of the state $|x,+1\rangle$ is *slowed* by collective effects; see Appendix A. As in the case of the center-of-mass motion, the amplitudes **b**, **c**, and **d** depend on the specific geometry of the laser excitation.

In the following section we turn to a detailed mathematical analysis of the two-ion model. Further examples and results will be presented in Sec. V.

III. MODEL

We consider two ions confined in a three-dimensional harmonic trap, interacting with a laser field. The master equation for the density operator of both the internal and external degrees of freedom of the ions can be derived after eliminat-

ing the quantized electromagnetic reservoir, resulting in

$$\dot{\rho}=\left(-\frac{i}{\hbar}h_{\rm eff}\rho+\frac{i}{\hbar}\rho h_{\rm eff}^{\dagger}\right)+L^{\rm rec}\rho. \tag{17}$$

Here $h_{\rm eff}$ is an effective non-Hermitian Hamiltonian that includes both the free effective Hamiltonian $H_{\rm eff}$ and the interaction $H_{\rm L}$ with the laser

$$h_{\rm eff}=H_{\rm eff}+H_{\rm L} \tag{18}$$

$$H_{\rm eff}=H_A+H_{\rm ext}+H_{11}+H_{12}, \tag{19}$$

and $L^{\rm rec}\rho$ is the recycling term related to spontaneous emission. In the following subsections we give the expressions for each of the Hamiltonians appearing in Eq. (18), as well as for the recycling term.

A. External degrees of freedom

In the absence of a laser field, the dynamics of the ions is determined by the external harmonic potential and the Coulomb repulsion. The Hamiltonian describing the external degrees of freedom of the ions is then given by

$$H_{\rm ext}=\sum_{\alpha=1,2}\left[\frac{\mathbf{p}^{(\alpha)2}}{2m}+\frac{1}{2}m(\nu_x^2x^{(\alpha)2}+\nu_y^2y^{(\alpha)2}+\nu_z^2z^{(\alpha)2})\right]+\frac{e^2}{4\pi\epsilon_0|\mathbf{x}^{(1)}-x^{(2)}|}. \tag{20}$$

Here m is the ion mass; e is the charge; $\nu_{x,y,z}$ are the trap frequencies along the x, y, and z, respectively; and $\mathbf{x}^{(\alpha)}\equiv(x^{(\alpha)},y^{(\alpha)},z^{(\alpha)})$ and $\mathbf{p}^{(\alpha)}$ are position and momentum operators of ion α, respectively.

Here we are interested in the last stages of laser cooling. In this situation, the ions undergo small oscillations around their (classical) equilibrium positions. If we assume that the trap frequency along the z axis is smaller than each of the other two frequencies ($\nu_z<\nu_{x,y}$), in equilibrium the ions will lie on the z axis, as given in [Eq. (8)]. By expanding the Coulomb potential around the equilibrium position and keeping terms up to second order in small displacements around these positions, Hamiltonian $H_{\rm ext}$ becomes (up to a constant corresponding to the minimum value of the potential at the equilibrium point)

$$H_{\rm ext}=\frac{\mathbf{P}'^2}{2m}+\frac{1}{2}m\sum_{u=x,y,z}\nu_u^2R_u'^2+\frac{\mathbf{p}'^2}{2m}+\frac{1}{2}m\sum_{u=x,y,z}\nu_{ru}^2(r_u'-r_{u0}')^2. \tag{21}$$

Here, $\mathbf{R}'$ and $\mathbf{r}'$ are the center-of-mass and relative position operators defined in Eq. (6), $\mathbf{P}'$ and $\mathbf{p}'$ are the corresponding conjugate momenta, and $\mathbf{r}_0'$ is the relative position at the equilibrium point, as given in Sec. II B. Thus, the motion can be described in terms of six modes, which are decoupled in the absence of other interactions. The eigenfrequencies for the center-of-mass modes coincide with the original trap frequencies, whereas those for the relative modes are $\nu_{rx,ry}=\sqrt{\nu_{x,y}^2-\nu_z^2}$, $\nu_{rz}=\sqrt{3}\nu_z$.

Quantizing the six harmonic oscillators, we introduce creation and annihilation operators $b_{ru}^{\dagger},b_{ru}$ $(u=x,y,z)$ for the modes of relative motion, which allows us to express

$$r_u'=r_{0u}'+\sqrt{\frac{\hbar}{2m\nu_{ru}}}(b_{ru}^{\dagger}+b_{ru}) \tag{22}$$

and $b_u^{\dagger},b_u$ $(u=x,y,z)$ for the center-of-mass motion, which results in

$$R_u'=\sqrt{\frac{\hbar}{2m\nu_u}}(b_u^{\dagger}+b_u). \tag{23}$$

Disregarding the constant term, we obtain

$$H_{\rm ext}=\frac{m}{2}\sum_{u=x,y,z}\nu_u^2b_u^{\dagger}b_u+\frac{m}{2}\sum_{u=x,y,z}\nu_{ru}^2b_{ru}^{\dagger}b_{ru}. \tag{24}$$

B. Internal degrees of freedom

We assume that the internal structure of the ions can be described as a two-level system. Its ground and excited state are separated by $\hbar\omega_0$ and are possibly degenerate. We will denote by $k\equiv\omega_0/c$ the corresponding wave number. These levels are excited by a laser field of frequency $\omega_{\rm L}$ close to ω_0. Using a frame rotating at the laser frequency, the free Hamiltonian for the internal degrees of freedom of the ions is

$$H_A=-\hbar\Delta\sum_{\alpha=1,2}P_e^{(\alpha)}, \tag{25}$$

where $P_e^{(\alpha)}=\Sigma_m|e,m\rangle_{\alpha\alpha}\langle e,m|$ is the projector onto the excited states of atom α, and $\Delta=\omega_{\rm L}-\omega_0$ is the laser detuning. The non-Hermitian Hamiltonian

$$H_{11}=-i\hbar\gamma\sum_{\alpha=1,2}P_e^{\alpha} \tag{26}$$

describes the decrease of the excited states population due to spontaneous emission for each of the two ions, with 2γ the spontaneous decay rate.

Although the formalism developed in this paper applies to any particular internal transition, we will focus most of our discussion on a simple situation corresponding to a $j_g=0\rightarrow j_e=1$ transition. This system is the simplest one that allows us to study different laser polarizations. The atomic internal states are then $|g\rangle$ and $|e,m\rangle$ $(m=-1,0,1)$. Using a Cartesian basis, the excited state can also be expressed as $|e_z\rangle=|1,0\rangle$, $|e_x\rangle=(|1,-1\rangle-|1,1\rangle)/\sqrt{2}$, $|e_y\rangle=i(|1,-1\rangle+|1,1\rangle)/\sqrt{2}$.

C. Atom-laser interaction

In the dipole and rotating-wave approximation, the interaction of the laser light with the ions is given by

$$H_{\rm L}=-\sum_{\alpha=1,2}\mathbf{E}^{(+)}(\mathbf{x}^{(\alpha)})\cdot\boldsymbol{\mu}^{(\alpha)}+\text{H.c.}, \tag{27}$$

where $\mathbf{E}^{(+)}(\mathbf{x})$ is the positive-frequency part of the laser field at position $\mathbf{x}$, and $\boldsymbol{\mu}^{(\alpha)}$ is the dipole moment of ion α.

Defining, as usual, the atomic excitation operator for atoms α as $\mathbf{D}^{(\alpha)}=P_e^{(\alpha)}\boldsymbol{\mu}^{(\alpha)}P_g^{(\alpha)}/|_\alpha\langle e\|\boldsymbol{\mu}_\alpha^{(\alpha)}\|g\rangle_\alpha|$, we express the atom-laser Hamiltonian in the general form

$$H_{\mathrm{L}}=\hbar\sum_{\alpha=1,2}\mathbf{V}(\mathbf{x}^{(\alpha)})\cdot\mathbf{D}^{(\alpha)}+\mathrm{H.c.} \tag{28}$$

By keeping unspecified the vector $\mathbf{V}$, our formalism will be valid for any laser configuration. However, for most of our discussion we will assume that the laser beam configuration corresponds to a plane traveling wave with linear polarization along the u axis. In this case,

$$\mathbf{V}(\mathbf{x})=\frac{\Omega}{2}e^{i\mathbf{k}_{\mathrm{L}}\cdot\mathbf{x}}\hat{\mathbf{e}}_u, \tag{29}$$

where $\mathbf{k}_{\mathrm{L}}$ is the laser wave vector, $\hat{\mathbf{e}}_u$ is the unit vector along the u direction, and Ω is the Rabi frequency.

D. Dipole-dipole interaction

The dipole-dipole interaction part of Hamiltonian (18) is given by

$$H_{12}=-i\hbar\gamma\sum_{\alpha\neq\beta}[f(d)\mathbf{D}^{(\alpha)}\cdot\mathbf{D}^{(\beta)\dagger}+g(d)(\mathbf{D}^{(\alpha)}\cdot\hat{\mathbf{r}})(\mathbf{D}^{(\beta)\dagger}\cdot\hat{\mathbf{r}})], \tag{30}$$

which results from the elimination of the quantized electromagnetic reservoir. It describes the atom-atom interaction when one of the atoms is in the ground state and the other in an excited state. In (30),

$$\mathbf{r}=\mathbf{x}^{(1)}-\mathbf{x}^{(2)},\quad \hat{\mathbf{r}}=\frac{\mathbf{r}}{|r|},\quad d=k|\mathbf{r}|, \tag{31}$$

and f and g are the familiar functions

$$f(d)=\tfrac{3}{2}\left[\sin(d)\left(\frac{1}{d}-\frac{1}{d^3}\right)+\cos(d)\frac{1}{d^2}\right]+i\tfrac{3}{2}\left[\cos(d)\left(-\frac{1}{d}+\frac{1}{d^3}\right)+\sin(d)\frac{1}{d^2}\right], \tag{32a}$$

$$g(d)=\tfrac{3}{2}\left[\sin(d)\left(-\frac{1}{d}+\frac{3}{d^3}\right)-\cos(d)\frac{3}{d^2}\right]+i\tfrac{3}{2}\left[\cos(d)\left(\frac{1}{d}-\frac{3}{d^3}\right)-\sin(d)\frac{3}{d^2}\right]; \tag{32b}$$

cf. [23].

Dipole-dipole interaction causes level shifts and modifications in the spontaneous-emission rates (i.e., in the level widths). This is very easy to show when the atoms are fixed (for example) at their equilibrium positions. To this aim we replace the operators d and $\hat{\mathbf{r}}$ in (30) with c numbers. Setting $a\equiv kr_0$ (r_0 being the inter-ion distance in equilibrium), and taking into account that in equilibrium the ions lie on the z axis, we obtain

$$H_{12}^{(0)}=-i\hbar\gamma\sum_{\alpha\neq\beta}[f(a)\mathbf{D}^{(\alpha)}\cdot\mathbf{D}^{(\beta)\dagger}+g(a)D_z^{(\alpha)}D_z^{(\beta)\dagger}]. \tag{33}$$

We denote by $|a;b\rangle\equiv|a\rangle_1|b\rangle_2$ the state in which atom 1 is in state $|a\rangle$ and atom 2 is in state $|b\rangle$. Let us consider the specific case of a $j_g=0\rightarrow j_e=1$ transition. Then there is a unique ground state $|g;g\rangle$, and the action of the Cartesian components of the dipole moment operators is $D_u^{(1)}|g;b\rangle=|e_u;b\rangle$, $u=x,y,z$, and similarly for atom 2 ($u=x,y,z$). Hence the states $|g;g\rangle$, $|u,\pm\rangle\equiv(|e_u;g\rangle\pm|g;e_u\rangle)/\sqrt{2}$, and $|e_i;e_u\rangle$ are eigenstates of $H_A+H_{11}+H_{12}^{(0)}$, with respective eigenvalues 0, $\hbar[-\Delta-i\gamma\mp i\gamma(f(a)+\delta_{uz}g(a))]$, and $\hbar(-2\Delta-i2\gamma)$ [see Eq. (9)]. Thus, the imaginary parts of $f(a)$ and $g(a)$ result in level shifts, while their real parts modify the lifetimes of the singly excited states. In particular, in the limit of small distance $a\rightarrow0$, the $|u,-\rangle$ states become metastable since $\lim_{a\rightarrow0}\mathrm{Re}[f(a)]=1$ and $\lim_{a\rightarrow0}\mathrm{Re}[g(a)]=0$ (cf. Fig. 2). We define

$$E_{u,\pm1}\equiv-\hbar\Delta\pm\delta E_u, \tag{34a}$$

$$\delta E_u\equiv\hbar\gamma\,\mathrm{Im}[f(a)+\delta_{uz}g(a)], \tag{34b}$$

and

$$\gamma_{u,\pm1}\equiv\gamma\pm\gamma\,\mathbf{Re}[f(a)+\delta_{uz}g(a)]. \tag{35}$$

E. Recycling term

The last term of master equation (17) is

$$L^{\mathrm{rec}}\rho=2\gamma\frac{3}{8\pi}\int d\Omega_{\hat{\mathbf{k}}}\sum_{\lambda=1,2}\sum_{\alpha,\beta=1,2}e^{-i\mathbf{k}\cdot\mathbf{x}^{(\alpha)}}[\boldsymbol{\epsilon}^{\lambda}(\hat{\mathbf{k}})\cdot\mathbf{D}^{(\alpha)\dagger}]\rho[\boldsymbol{\epsilon}^{\lambda}(\hat{\mathbf{k}})\cdot\mathbf{D}^{(\beta)}]e^{i\mathbf{k}\cdot\mathbf{x}^{(\beta)}}, \tag{36}$$

where $\int d\Omega_{\hat{\mathbf{k}}}$ stands for integration over the unit sphere, and $\boldsymbol{\epsilon}^1(\hat{\mathbf{k}}),\boldsymbol{\epsilon}^2(\hat{\mathbf{k}})$ form a set of polarization vectors orthogonal to $\hat{\mathbf{k}}$. This ''recycling'' term describes the return of an atom from an excited to a ground state, accompanied by a momentum kick. It can be rewritten as

$$L^{\mathrm{rec}}\rho=2\gamma\frac{3}{8\pi}\int d\Omega_{\hat{\mathbf{k}}}\sum_{\alpha,\beta=1,2}e^{-i\mathbf{k}\cdot\mathbf{x}^{(\alpha)}}[\mathbf{D}^{(\alpha)^+}\cdot\rho\mathbf{D}^{(\beta)}-(\hat{\mathbf{k}}\cdot\mathbf{D}^{(\alpha)^+})\rho(\hat{\mathbf{k}}\cdot\mathbf{D}^{(\beta)})]e^{i\mathbf{k}\cdot\mathbf{x}^{(\beta)}}. \tag{37}$$

IV. RATE EQUATIONS

Master equation (17) is difficult to solve, even numerically. However, if one restricts it to the low-intensity limit it can be converted into a set of rate equations, after elimination of the excited internal levels. This equation can be further simplified if one takes into account that in the final stages of laser cooling the oscillation amplitudes of the ions are much smaller than the laser wavelength (Lamb-Dicke limit).

In the low-intensity limit (small Rabi frequency Ω of the incident laser light, so that there are no saturation effects) the trap populations evolve much slower than the coherences between trap states or the internal degrees of freedom, which therefore can be adiabatically eliminated. This leads in second-order perturbation theory to a rate equation for the trap populations of the form (1). There the transition rates $\Gamma_{\mathbf{m}\leftarrow\mathbf{n}}$ are given in Eq. (12), where we have defined $H_{\rm eff}=H_A+H_{\rm ext}+H_{11}+H_{12}$ and $E_{\mathbf{n}}$ is the unperturbed energy of the atomic ground state with oscillator state $|\mathbf{n}\rangle$: $H_{\rm eff}|g;g\rangle|\mathbf{n}\rangle=E_{\mathbf{n}}|g;g\rangle|\mathbf{n}\rangle$.

In the Lamb-Dicke limit, the Lamb-Dicke parameters defined in (13) are much smaller than 1. It is therefore convenient to expand the rates $\Gamma_{\mathbf{m}\leftarrow\mathbf{n}}$ in the η's and keep the lowest-order contributions. The leading contribution in expression (12) is second order in such an expansion. In order to get that, it suffices to expand up to first order the three operators: $e^{-i\mathbf{k}\cdot\mathbf{x}^{(\alpha)}}$, $1/(H_{\rm eff}-E_{\mathbf{n}})$, and H_L. In the following we carry out that task. First,

$$e^{-i\mathbf{k}\cdot\mathbf{x}^{(1,2)}}=e^{-i\mathbf{k}\cdot\mathbf{X}^{(1,2)}}\left[1-i\sum_u \hat{k}_u\frac{1}{\sqrt{2}}[\eta_u(b_u^\dagger+b_u)\pm\eta_{ru}(b_{ru}^\dagger+b_u)]\right]. \tag{38}$$

In order to get the result for $1/(H_{\rm eff}-E_{\mathbf{n}})$ we use

$$\frac{1}{H_{\rm eff}-E_{\mathbf{n}}}=\frac{1}{H_{\rm eff}^{(0)}-E_{\mathbf{n}}}+\frac{1}{H_{\rm eff}^{(0)}-E_{\mathbf{n}}}(-H_{12}^{(1)})\frac{1}{H_{\rm eff}^{(0)}-E_{\mathbf{n}}}+\cdots, \tag{39}$$

where

$$H_{\rm eff}^{(1)}=-i\hbar\gamma\sum_{\alpha\neq\beta}\sum_u[\delta_{u,z}(af'(a)\mathbf{D}^{(\alpha)}\cdot\mathbf{D}^{(\beta)^\dagger}+ag'(a)D_z^{(\alpha)}D_z^{(\beta)^\dagger})+(1-\delta_{u,z})g(a)(D_u^{(\alpha)}D_z^{(\beta)^\dagger}+D_z^{(\alpha)}D_u^{(\beta)^\dagger})]\sqrt{2}\frac{\eta_{ru}}{a}(b_{ru}^\dagger+b_{ru}). \tag{40}$$

Note that this last is an expansion in terms of the parameter $\zeta_u=\eta_{ru}/a$ [see Eq. (10)] rather than η_{ru}.

Finally, we find for the atom-laser interaction

$$H_{\rm L}^{(0)}=\hbar\sum_{\alpha=1,2}\mathbf{V}(\mathbf{X}^{(\alpha)})\cdot\mathbf{D}^{(\alpha)}+\text{H.c}, \tag{41a}$$

$$H_{\rm L}^{(1)}=\hbar\sum_{\alpha=1,2}(\mathbf{q}^{(\alpha)}\cdot\nabla)\mathbf{V}(\mathbf{X}^{(\alpha)})\cdot\mathbf{D}^{(\alpha)}+\text{H.c.}, \tag{41b}$$

where $\mathbf{q}^{(\alpha)}\equiv(\mathbf{x}^{(\alpha)}-\mathbf{X}^{(\alpha)})$; i.e.,

$$q_u^{(1,2)}=\frac{1}{\sqrt{2}}\left(\frac{\eta_u}{k}(b_u^\dagger+b_u)\pm\frac{\eta_{ru}}{k}(b_{ru}^\dagger+b_{ru})\right). \tag{42}$$

Substituting all these results of the expansion in the expression for the rates, we find Eq. (14). As stated in Sec. II, the vectors **b**, **c**, and **d** appearing in this expression have a very intuitive interpretation in terms of physical processes, where one laser photon is absorbed and spontaneously reemitted.

Next we evaluate the matrix elements involved in the definitions of the vectors **b**, **c**, and **d** given in (16). To this aim we first note that the rates $\Gamma_{\mathbf{m}\leftarrow\mathbf{n}}$ are different from zero only if **m** differs from **n** by ±1 in exactly one out of the six vibrational modes: $|\mathbf{m}\rangle\equiv|n_x\pm1\ n_yn_zn_{rx}n_{ry}n_{rz}\rangle$, etc. Thus we concentrate on transitions that change one specific mode p $(=x,y,z,rx,ry,rz)$; i.e., for an initial trap state $|\mathbf{n}\rangle=|n_xn_yn_zn_{rx}n_{ry}n_{rz}\rangle$, the final state is assumed to be $|\mathbf{m}\rangle=|\cdots n_p\pm1\cdots\rangle$. For the sake of a short notation, we find it convenient to denote by u the corresponding direction of this mode. That is, for $p=x$ or $p=rx$, we will have $u=x$, etc. Furthermore, we will use the vector

$$\tilde{\mathbf{d}}^{(\alpha)}\equiv\langle\mathbf{m}|\langle g;g|\mathbf{D}^{(\alpha)^+}kq_u^{(\alpha)}\frac{1}{H_{\rm eff}^{(0)}-E_{\mathbf{n}}}H_{\rm L}^{(0)}|g;g\rangle|\mathbf{n}\rangle \tag{43}$$

instead of $\mathbf{d}^{(\alpha)}$ (note that $\mathbf{d}^{(\alpha)}=\hat{k}_u\tilde{\mathbf{d}}^{(\alpha)}$, while $\tilde{\mathbf{d}}^{(\alpha)}$ does not depend on the integration variable $\hat{\mathbf{k}}$).

Upon inserting projectors onto the subspace of singly excited states, in vectors $\mathbf{b}^{(\alpha)}$, $\mathbf{c}^{(\alpha)}$, and $\tilde{\mathbf{d}}^{(\alpha)}$ there can be identified the contributions belonging to the various intermediate internal states $|j,s\rangle$:

$$\mathbf{b}^{(\alpha)}=\frac{1}{2\sqrt{2}}\eta_p\langle\mathbf{m}|(b_p+b_p^\dagger)|\mathbf{n}\rangle\sum_{j=x,y,z}\sum_{s=\pm1}\hat{e}_j s^{\alpha-1}\frac{\frac{1}{k}\left(\frac{\partial V_j}{\partial u}(\mathbf{X}^{(1)})+[\mathrm{sg}(p)]s\frac{\partial V_j}{\partial u}(\mathbf{X}^{(2)})\right)}{E_{j,s}/\hbar-i\gamma_{j,s}\pm\nu_p}, \tag{44a}$$

$$\tilde{\mathbf{d}}^{(\alpha)}=\frac{1}{2\sqrt{2}}\eta_p\langle\mathbf{m}|(b_p+b_p^\dagger)|\mathbf{n}\rangle\sum_{j=x,y,z}\sum_{s=\pm1}\hat{e}_j[\mathrm{sg}(p)s]^{\alpha-1}\frac{V_j(\mathbf{X}^{(1)})+sV_j(\mathbf{X}^{(2)})}{E_{j,s}/\hbar-i\gamma_{j,s}}, \tag{44b}$$

where the sign in $\mathrm{sg}(p)$ distinguishes between center-of-mass and relative motion:

$$\mathrm{sg}(p)\equiv\begin{cases}1 & \text{if } p\in\{x,y,z\}\\ -1 & \text{if } p\in\{rx,ry,rz\}.\end{cases} \tag{45}$$

The vectors $\mathbf{c}^{(\alpha)}=0$ are nonzero only for relative motion. If $p=rz$ we have

$$\mathbf{c}^{(\alpha)}=\frac{1}{\sqrt{2}}\eta_p\langle\mathbf{m}|(b_p+b_p^\dagger)|\mathbf{n}\rangle\sum_{j=x,y,z}\sum_{s=\pm1}\hat{e}_j s^\alpha i\gamma(f'(a)+\delta_{jz}g'(a))\frac{V_j(\mathbf{X}^{(1)})+sV_j(\mathbf{X}^{(2)})}{(E_{j,s}/\hbar-i\gamma_{j,s}\pm\nu_p)(E_{j,s}/\hbar-i\gamma_{j,s})}, \tag{46}$$

whereas if $p=rx,ry$,

$$\mathbf{c}^{(\alpha)}=\frac{1}{\sqrt{2}}\eta_p\langle\mathbf{m}|(b_p+b_p^\dagger)|\mathbf{n}\rangle\sum_{s=\pm1}s^\alpha i\gamma\frac{g(a)}{a}\left(\hat{e}_u\frac{V_z(\mathbf{X}^{(1)})+sV_z(\mathbf{X}^{(2)})}{(E_{u,s}/\hbar-i\gamma_{u,s}\pm\nu_p)(E_{z,s}/\hbar-i\gamma_{z,s})}\right.$$
$$\left.+\hat{e}_z\frac{V_u(\mathbf{X}^{(1)})+sV_u(\mathbf{X}^{(2)})}{(E_{z,s}/\hbar-i\gamma_{z,s}\pm\nu_p)(E_{u,s}/\hbar-i\gamma_{u,s})}\right). \tag{47}$$

While the α dependence of the vectors $\mathbf{b}^{(\alpha)}$, $\mathbf{c}^{(\alpha)}$, and $\tilde{\mathbf{d}}^{(\alpha)}$ is nontrivial, simple rules hold for the terms involving singly excited states that are all symmetric ($s=1$) or all antisymmetric ($s=-1$). To show this we define

$$\mathbf{b}_s^{(\alpha)}=\frac{1}{2\sqrt{2}}\eta_p\langle\mathbf{m}|(b_p+b_p^\dagger)|\mathbf{n}\rangle\sum_{j=x,y,z}\hat{e}_j s^{\alpha-1}$$
$$\times\frac{\frac{1}{k}\left(\frac{\partial V}{\partial u}(\mathbf{X}^{(1)})+\mathrm{sg}[(p)s]\frac{\partial V}{\partial u}(\mathbf{X}^{(2)})\right)}{E_{j,s}/\hbar-i\gamma_{j,s}\pm\nu_p} \tag{48}$$

and similarly $\mathbf{c}_s^{(\alpha)}$, $\tilde{\mathbf{d}}_s^{(\alpha)}$. Then one finds

$$\mathbf{b}_s^{(2)}=s\mathbf{b}_s^{(1)},\quad \mathbf{c}_s^{(2)}=s\mathbf{c}_s^{(1)},\quad \tilde{\mathbf{d}}_s^{(2)}=\mathrm{sg}(p)s\tilde{\mathbf{d}}_s^{(1)}. \tag{49}$$

These relations will hold approximately for the vectors $\mathbf{b}^{(\alpha)}$, $\mathbf{c}^{(\alpha)}$, $\tilde{\mathbf{d}}^{(\alpha)}$ themselves if the laser is tuned to resonance (either central line or an upper or lower sideband) for some intermediate state $|j,s\rangle$.

V. DISCUSSION

In the following discussion it is first demonstrated how level shifts and lifetime modifications resulting from the zeroth-order dipole-dipole interaction $H_{12}^{(0)}$ show up in cooling and heating rates. As a next step, we investigate how the first-order dipole-dipole term $H_{12}^{(1)}$—the **c** contributions in Eq. (14)—can give rise to cooling or heating. Then we turn to the interferences of different processes.

In the examples, we mostly study single-plane traveling waves, e.g.,

$$\mathbf{V}(\mathbf{x})=\frac{\Omega}{2}\hat{\mathbf{e}}_x e^{ikz} \tag{50}$$

for a wave in z direction with a linear polarization in x direction, Ω being the Rabi frequency. In most examples below, the equilibrium distance of the ions are chosen 1/8 of the wavelength, i.e., $a=2\pi/8$. The trap frequencies are chosen in the strong binding regime: $\nu_x=120\gamma$, $\nu_y=100\gamma$, and $\nu_z=80\gamma$, which result in $\nu_{rx}=40\sqrt{5}\gamma\approx89.4\gamma$, $\nu_{ry}=60\gamma$, and $\nu_{rz}=80\sqrt{3}\gamma\approx138.6\gamma$. While the basic results have already been outlined in Sec. II, the following analysis aims at a deeper understanding of several more technical points.

A. Collective effects in sideband cooling and diffusion

Fig. 4 displays the cooling and heating coefficients A_{z-}, A_{z+} for the z component of center-of-mass motion in a plane traveling wave in the z direction, which is linearly polarized in the x direction. As pointed out in Sec. II D 1, for a small equilibrium distance ($a=2\pi/8$), each resonance is split into two lines, corresponding to the states $|x,s\rangle$, $s=\pm1$. They are shifted with respect to each other by $2\delta E_x/\hbar\approx5.12\gamma$. The $s=-1$ resonances are visibly narrower than the $s=+1$ ones since $\gamma_{x,-1}\approx0.12\gamma$ is much smaller than $\gamma_{x,+1}\approx1.88\gamma$. Their different heights result from three effects: (i) the different energy denominators account, at resonance, for a factor of $\gamma_{x,+1}^2$ and $\gamma_{x,-1}^2$, (ii) the laser field couples differently to $s=-1$ and $s=+1$ states; see (44a); and (iii) there are collective effects in the spontaneous deexcitation step that enhance or decrease the rates for the different processes. As discussed in Appendix A, this last effect is different for center-of-mass modes, as opposed to modes of relative motion, if a phonon is created or annihilated in the spontaneous deexcitation. For phonons of a center-of-mass mode, spontaneous emission from a state $|\cdot,+1\rangle$ is enhanced, and that from a state $|\cdot,-1\rangle$ is decreased, whereas for phonons of relative motion it is the other way around; namely, spontaneous emission from a state $|\cdot,-1\rangle$ is enhanced, and that from a state $|\cdot,+1\rangle$ is decreased. For the

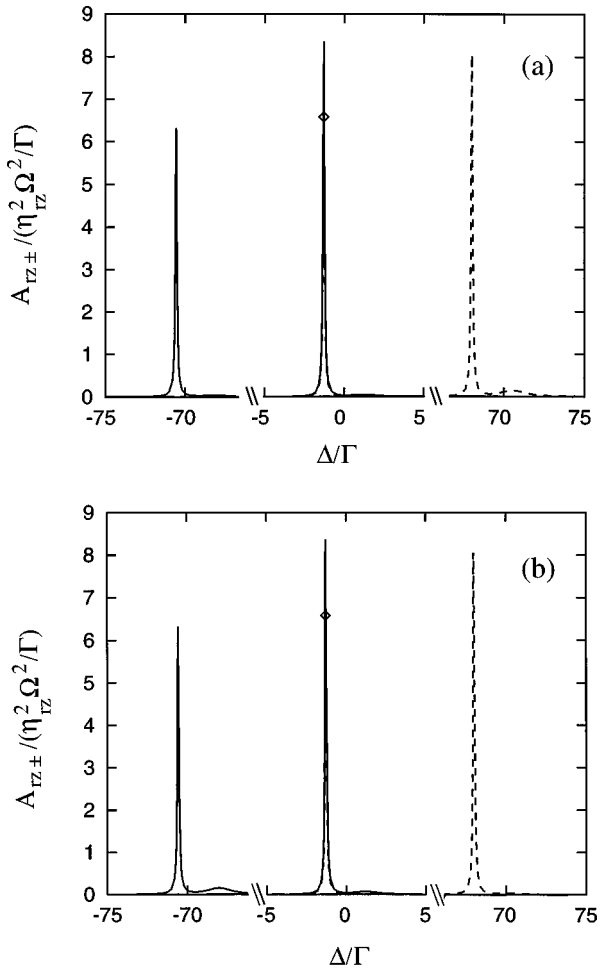

FIG. 7. Cooling and heating coefficients A_{rz-} (solid curve) and A_{rz+} (dashed curve) for the z component of relative motion. Laser configuration (a) $\mathbf{V}(\mathbf{x})=\hat{\mathbf{e}}_x e^{ikz}\Omega/2$; (b) $\mathbf{V}(\mathbf{x})=\hat{\mathbf{e}}_x(e^{ikz}-2e^{iky})\Omega/2$. $\diamond$ marks the height of the central peak of the dashed line. $\Gamma\equiv 2\gamma$.

central peaks in Fig. 4(b), e.g., the narrow line is higher than the broad one because of the different energy denominators; see (i) above. The difference in height is somewhat reduced by the collective effects [(iii) above]. But for a mode of relative motion, the last effect *increases* the difference because there it is the antisymmetric ($s=-1$) state that decays faster (if the deexcitation is accompanied by a phonon annihilation or creation). This is why the heights of the central peaks for narrow and broad resonances differ much less in Fig. 4(b) (center-of-mass motion) than, e.g., in Fig. 7(a) (relative motion).

B. Cooling via dipole-dipole terms

Since the amplitude resulting from the dipole-dipole interaction $\mathbf{c}^{(\alpha)}$ contains the vibrational frequency $\pm\nu_p$, it gives rise to, in general, different contributions to A_{p+} and A_{p-} if p is a mode of relative motion. Therefore, a net cooling (or a net heating) via these processes is possible. This was illustrated in Figs. 5(a) and 5(b) (see the discussion in Sec. II D 2). With the formalism developed in Sec. III C, we can now discuss in a more quantitative way the explanation given in Sec. II D 2 for the fact that the excitation without change of phonon number involves only the state $|x,+1\rangle$, not $|x,-1\rangle$; the excitation of the latter involves [see Eqs. (44b), (46), and (47)] $V_j(\mathbf{X}^{(1)})-V_j(\mathbf{X}^{(2)})$, which vanishes for the chosen configuration, namely, $\mathbf{V}(\mathbf{x})=\hat{\mathbf{e}}_x e^{iky}\Omega/2$. Similarly it can be shown with the help of Eq. (44a) that for mode ry there is a nonvanishing $\mathbf{b}$ contribution (the sideband cooling-heating amplitudes) involving only the states $|x,-1\rangle$, the excitation of which is accompanied by phonon creation or annihilation.

A qualitative difference between the two cases $p=rx$ in Fig. 5(a) and $p=rz$ in Fig. 5(b) arises from the fact that for $p=rz$, only one of the singly excited states is involved, but two in the case $p=rx$. In the first case, the relevant factor in (46) containing the laser detuning [cf. (34)] is

$$\frac{1}{(E_{x,+1}/\hbar-i\gamma_{x,+1}\pm\nu_{rz})(E_{x,+1}/\hbar-i\gamma_{x,+1})}. \tag{51}$$

When the laser is detuned so as to obtain $E_{x,+1}/\hbar=\mp\nu_{rz}$ (the upper or lower sideband resonance), this becomes

$$\frac{1}{-i\gamma_{x,+1}(\mp\nu_{rz}-i\gamma_{x,+1})}, \tag{52}$$

the modulus of which *does not* depend on the sign in front of ν_{rz}. In the second case, inserting $E_{z,+1}/\hbar=\mp\nu_{rx}$ into

$$\frac{1}{(E_{z,+1}/\hbar-i\gamma_{z,+1}\pm\nu_{rx})(E_{x,+1}/\hbar-i\gamma_{x,+1})} \tag{53}$$

[cf. (47)] yields

$$\frac{1}{-i\gamma_{z,+1}(-\gamma\,\mathrm{Re}(g(a))\mp\nu_{rx}-i\gamma_{x,+1})}, \tag{54}$$

the modulus of which *does* depend on the sign in front of ν_{rx}. As a result, the peaks in A_{p-} at the lower sideband and in A_{p+} at the upper one are of equal magnitude for $p=rz$ [Fig. 5(b)], but not for $p=rx$ [Fig. 5(a)].

The importance of the dipole-dipole induced amplitude $\mathbf{c}^{(\alpha)}$ in comparison with the other amplitudes $\mathbf{b}^{(\alpha)},\mathbf{d}^{(\alpha)}$ can be estimated as follows. For simplicity, let us assume that all terms involving the laser field and its derivatives are of equal order of magnitude. The amplitudes $\mathbf{b}^{(\alpha)}$ and $\mathbf{d}^{(\alpha)}$ of the sideband and diffusion processes have just one energy denominator; the amplitudes $\mathbf{c}^{(\alpha)}$ have two different energy denominators, at least one of which will always be out of resonance, and they have the matrix elements of H_{12} in the numerator. For $a\ll 1$, the latter are of the order of $9\gamma a^{-4}$. Hence, for a laser detuning that makes one of the energy denominators resonant, the resonant component of $\mathbf{c}^{(\alpha)}$ differs in magnitude from the same component of $\mathbf{b}^{(\alpha)}$ or $\mathbf{d}^{(\alpha)}$ (whichever is resonant), under the above assumption, roughly by a factor of $9\gamma/(\nu_p a^4)$. The denominator scales $\sim r_0^{5/2}$; therefore the process mediated by dipole-dipole interaction of Fig. 3(c) can be significant in the cooling process for small ion distances.

C. Discussion of interferences

Whenever there is more than one term contributing to the same Cartesian component in the total amplitude

$\mathbf{b}+\mathbf{c}-i\hat{k}_u\tilde{\mathbf{d}}$, there is the possibility of an interference of the processes involved. It is called a constructive interference if the net contribution to the transition rate is bigger than the sum of the contributions calculated separately from each of these processes, and a destructive one in the opposite case.

In the single-ion case, interference of the amplitudes for sideband and diffusion processes vanishes when the integral over all possible directions of spontaneous emission is performed. A similar argument holds for certain interferences in the two-ion case. Recall that each of the amplitudes **b**, **c**, and **d** is a sum of terms involving different intermediate states $|j,s\rangle$ [see Eqs. (44a), (44b), (46), and (47)] and deexcitation via different atoms α [see Eq. (15)]. The contributions belonging to a certain intermediate state obey the rules (49) with the appropriate sign s. For the two-ion case, the result of the integration over emission directions is given in Eqs. (A1) and (A2). With their help it can be shown that for $p\in\{rx,ry,rz\}$, processes involving intermediate states $|\cdot,s=\pm 1\rangle$ with different s do not interfere. For $p\in\{x,y,z\}$, two processes that both contribute to **b** (or both to **d**) do not interfere if they involve intermediate states with different symmetry s, while a process in **b** does not interfere with a process in **d** if they involve *the same* s.

In the strong binding limit $\gamma\ll\nu_p$, which is of interest here, at any central line or sideband resonance, all interferences between processes in the $\mathbf{b}^{(\alpha)}$, on the one hand, and the $\mathbf{d}^{(\alpha)}$, on the other hand, are insignificant in comparison to the corresponding squared amplitudes because of the presence of two different energy denominators, one of which will always be out of resonance in the interference term. Thus these interferences are suppressed by a factor of γ/ν_p if the laser-field dependent terms are again supposed to be of equal magnitude. Therefore, the only significant interferences seem to be the ones between a process in $\mathbf{c}^{(\alpha)}$ and another one in $\mathbf{b}^{(\alpha)}$ or $\mathbf{d}^{(\alpha)}$, if the parameter $9\gamma/(\nu_p a^4)$ derived above is not too small.

The influence of interferences shows up in Fig. 7(a), which displays the heating and cooling coefficients $A_{rz\pm}$ for the relative motion in the z direction as a function of laser detuning. The narrow peaks in A_{rz-} at the lower sideband and in A_{rz+} at the upper one involve the excitation of the $|x,-1\rangle$ state. The difference in height of these two peaks is due to the fact that in A_{rz-}, at the lower sideband, there is *destructive* interference of the ordinary sideband cooling process due to dipole-dipole interaction, while the peak in A_{rz+} at the upper sideband is enhanced by *constructive* interference.

The occurrence of interference is discussed in more detail in Appendix B. In particular, it is investigated there to what extent the laser configuration has an influence on whether the interference is destructive or constructive.

VI. CONCLUSIONS

In this paper we have studied the effects of dipole-dipole interaction in laser cooling. We have considered the case of two ions confined in a three-dimensional harmonic trap interacting with a laser field. We have derived a set of rate equations that describe the cooling process in the low-intensity and Lamb-Dicke limits. For inter-ion distances smaller than the wavelength of the internal transition, the effects of dipole-dipole interaction are reflected in the cooling process. First, this interaction causes level shifts and modifies the decay rates. Second, the gradient of the dipole-dipole potential also changes the motional state. The first effect results in the appearance of pairs of sidebands in the coefficients $A_\pm$ (i.e., in the cooling rates), each of them corresponding to cooling via the excitation of a symmetric or antisymmetric state. The second effect leads to novel phenomena, such as the possibility of transverse cooling or interferences with processes resulting from dipole-dipole interaction. Typically this effect tends to be a small correction. For the center-of-mass modes, only the first effect shows up. For the relative motion modes both effects occur. We have illustrated these phenomena in a particular case: an internal $j_g=0\rightarrow j_e=1$ transition. We have considered excitation by laser fields with linear polarization, with different geometries. The results that we have shown will occur in any given transition. While the equilibrium distance of $\lambda/8$ chosen in our examples is small compared to current experimental values, we assume that experimental progress in ion trapping will allow us to observe the predicted effects in the future. On the other hand, we believe that the present analysis may be useful to other studies of laser cooling with neutral atoms.

Finally, we would like to comment on the fact that throughout this paper we have considered a time-independent harmonic trap, whereas in the rf traps used in experiments (e.g., [9]) the trapping potential is time-dependent, leading to the well-known micromotion. The frequency of this micromotion, Ω, is typically much larger than the resulting effective trap frequencies ν_j (except for experiments that explore the boundary of the stability region of such a trap) and also larger than the frequencies of relative motion, ν_{rj}, $j=x,y,z$. An analysis of the influence of micromotion on the laser cooling of a single ion [25] has shown that the basic features remain the same, but additional sidebands shifted by Ω are introduced. We expect this to hold in the two-ion case, too. All these sidebands are well separated because of the relations $\Omega\gg\nu_j,\nu_{rj}\gg\gamma$, where the last inequality is the sideband limit assumed at the outset. Therefore, for laser detunings below Ω, the features discussed in this paper should be found even in a trap with micromotion. For larger detuning, additional resonances will show up.

ACKNOWLEDGMENTS

A.W.V. acknowledges financial support from the Deutsche Forschungsgemeinschaft and thanks JILA and the University of Innsbruck for hospitality. Work at JILA was supported in part by NSF. Research at the University of Innsbruck is supported in part by the Österreichische Fonds zur Förderung der wissenschaftlichen Forschung.

APPENDIX A: EVALUATION OF INTEGRALS

In this appendix we evaluate the integral over the direction of spontaneous emission in our expressions for cooling and heating rates and discuss the enhancement or slowing

down of decay in the deexcitation step resulting in the limit $a \to 0$. In the following, the abbreviation $\mathbf{v}^{(\alpha)} \equiv \mathbf{b}^{(\alpha)} + \mathbf{c}^{(\alpha)}$ is used.

Upon evaluating the integral, the transition rate (12) becomes (i) in the case $u = z$, i.e., for the z component of relative or center-of-mass motion

$$\begin{aligned}\Gamma_{\mathbf{m}\leftarrow\mathbf{n}} = 2\gamma \frac{3}{8\pi} \int d\Omega_{\hat{\mathbf{k}}} \left(\left| \sum_{\alpha=1,2} e^{-i\mathbf{k}\cdot\mathbf{X}^{(\alpha)}} (\mathbf{v}^{(\alpha)} - i\hat{k}_u \tilde{\mathbf{d}}^{(\alpha)}) \right|^2 - \left| \hat{\mathbf{k}} \cdot \sum_{\alpha=1,2} e^{-i\mathbf{k}\cdot\mathbf{X}^{(\alpha)}} (\mathbf{v}^{(\alpha)} - i\hat{k}_u \tilde{\mathbf{d}}^{(\alpha)}) \right|^2 \right)$$

$$\begin{aligned} &= 2\gamma \left(\sum_{\alpha=1,2} \left\{ |\mathbf{v}^{(\alpha)}|^2 + \frac{2}{5} |\tilde{\mathbf{d}}^{(\alpha)}|^2 - \frac{1}{5} |\tilde{d}_z^{(\alpha)}|^2 \right\} + 2\ \mathrm{Re}[f(a)]\mathrm{Re}(\mathbf{v}^{(1)} \cdot \mathbf{v}^{(2)*}) + 2\ \mathrm{Re}[g(a)]\mathrm{Re}(v_z^{(1)} v_z^{(2)*}) \right. \\ &\quad + \frac{3}{8}(c_2 + c_4) 2\ \mathrm{Re}(\tilde{\mathbf{d}}^{(1)} \cdot \tilde{\mathbf{d}}^{(2)*}) - \frac{3}{8}(-c_2 + 3c_4) 2\ \mathrm{Re}(\tilde{d}_z^{(1)} \tilde{d}_z^{(2)*}) \\ &\quad + \frac{3}{8}(s_1 + s_3) 2\ \mathrm{Re}(\mathbf{v}^{(1)} \cdot \tilde{\mathbf{d}}^{(2)*} - \mathbf{v}^{(2)} \cdot \tilde{\mathbf{d}}^{(1)*}) \\ &\quad \left. + \frac{3}{8}(-s_1 + 3s_3) 2\ \mathrm{Re}(-v_z^{(1)} \tilde{d}_z^{(2)*} + v_z^{(2)} \tilde{d}_z^{(1)*}) \right) \end{aligned} \tag{A1}$$

or (ii) in the case $u = x, y$

$$\Gamma_{\mathbf{m}\leftarrow\mathbf{n}} = 2\gamma \frac{3}{8\pi} \int d\Omega_{\hat{\mathbf{k}}} \left(\left| \sum_{\alpha=1,2} e^{-i\mathbf{k}\cdot\mathbf{X}^{(\alpha)}} (\mathbf{v}^{(\alpha)} - i\hat{k}_u \tilde{\mathbf{d}}^{(\alpha)}) \right|^2 - \left| \hat{\mathbf{k}} \cdot \sum_{\alpha=1,2} e^{-i\mathbf{k}\cdot\mathbf{X}^{(\alpha)}} (\mathbf{v}^{(\alpha)} - i\hat{k}_u \tilde{\mathbf{d}}^{(\alpha)}) \right|^2 \right)$$

$$\begin{aligned} &= 2\gamma \left(\sum_{\alpha=1,2} \left\{ |\mathbf{v}^{(\alpha)}|^2 + \frac{2}{5} |\tilde{\mathbf{d}}^{(\alpha)}|^2 - \frac{1}{5} |\tilde{d}_u^{(\alpha)}|^2 \right\} + 2\ \mathrm{Re}[f(a)]\mathrm{Re}(\mathbf{v}^{(1)} \cdot \mathbf{v}^{(2)*}) + 2\ \mathrm{Re}[g(a)]\mathrm{Re}(v_z^{(1)} v_z^{(2)*}) \right. \\ &\quad + \frac{3}{32}(3c_0 - 2c_2 - c_4) 2\ \mathrm{Re}(\tilde{\mathbf{d}}^{(1)} \cdot \tilde{\mathbf{d}}^{(2)*}) - \frac{3}{32}(-c_0 + 6c_2 - 5c_4) 2\ \mathrm{Re}(\tilde{d}_z^{(1)} \tilde{d}_z^{(2)*}) \\ &\quad - \frac{3}{16}(c_0 - 2c_2 + c_4) 2\ \mathrm{Re}(\tilde{d}_u^{(1)} \tilde{d}_u^{(2)*}) \\ &\quad \left. + \frac{3}{8}(s_1 - s_3) 2\ \mathrm{Re}(-v_z^{(1)} \tilde{d}_u^{(2)*} + v_z^{(2)} \tilde{d}_u^{(1)*} - v_u^{(1)} \tilde{d}_z^{(2)*} + v_u^{(2)} \tilde{d}_z^{(1)*}) \right) \end{aligned} \tag{A2}$$

where

$$c_0 \equiv \int_{-1}^{1} \cos(ax)\, dx, \tag{A3a}$$

$$c_2 \equiv \int_{-1}^{1} x^2 \cos(ax)\, dx, \tag{A3b}$$

$$c_4 \equiv \int_{-1}^{1} x^4 \cos(ax)\, dx, \tag{A3c}$$

$$s_1 \equiv \int_{-1}^{1} x \sin(ax)\, dx, \tag{A3d}$$

$$s_3 \equiv \int_{-1}^{1} x^3 \sin(ax)\, dx. \tag{A3e}$$

In terms of these,

$$\mathrm{Re}[f(a)] = \frac{3}{8}(c_0 + c_2) = 1 - \frac{1}{5}a^2 + \cdots ,$$

$$\mathrm{Re}[f(a)+g(a)]=\frac{3}{4}(c_0-c_2)=1-\frac{1}{10}a^2+\cdots .$$

Note that for $\mathbf{v}^{(2)}=\pm\mathbf{v}^{(1)}$, which holds approximately at a resonance for some state $|u,\pm1\rangle$,

$$2\gamma\left(\sum_{\alpha=1,2}|\mathbf{v}^{(\alpha)}|^2+2\ \mathrm{Re}[f(a)]\mathrm{Re}(\mathbf{v}^{(1)}\cdot\mathbf{v}^{(2)*})+2\ \mathrm{Re}[g(a)]\mathrm{Re}(v_z^{(1)}v_z^{(2)*})\right)=2\gamma_{x,\pm1}(|v_x^{(1)}|^2+|v_y^{(1)}|^2)+2\gamma_{z,\pm1}|v_z^{(1)}|^2, \tag{A4}$$

which makes apparent the modified decay rate of the state $|u,\pm1\rangle$. It simply means that the final spontaneous emission (without change of the motional quantum number) in processes (a) and (c) of Fig. 3 occurs at a rate of the appropriate $2\gamma_{u,s}$.

For the final spontaneous emission *with* change of the motional quantum number in process (b) of Fig. 3, a similar phenomenon occurs. Here we consider center of mass and relative motion separately. If $\Gamma_{\mathbf{m}\leftarrow\mathbf{n}}$ describes the creation or annihilation of a center-of-mass phonon (i.e., $m_u=n_u\pm1$ for a certain $u\in\{x,y,z\}$) and the laser is tuned to resonance for some state $|\cdot,\pm1\rangle$, then $\tilde{\mathbf{d}}^{(2)}=\pm\tilde{\mathbf{d}}^{(1)}$ holds approximately. We further distinguish between $u=z$ and $u=x,y$.

(i) For $u=z$, Eq. (A1) contains

$$2\gamma\left(\sum_{\alpha=1,2}\left[\frac{2}{5}|\tilde{\mathbf{d}}^{(\alpha)}|^2-\frac{1}{5}|\tilde{d}_z^{(\alpha)}|^2\right]+\frac{3}{8}(c_2+c_4)2\ \mathrm{Re}(\tilde{\mathbf{d}}^{(1)}\cdot\tilde{\mathbf{d}}^{(2)*})-\frac{3}{8}(-c_2+3c_4)2\ \mathrm{Re}(\tilde{d}_z^{(1)}\tilde{d}_z^{(2)*})\right)$$
$$=2\gamma\left[\frac{4}{5}|\tilde{\mathbf{d}}^{(1)}|^2\left(1\pm\frac{15}{16}(c_2+c_4)\right)-\frac{2}{5}|\tilde{d}_z^{(1)}|^2\left(1\pm\frac{15}{8}(-c_2+3c_4)\right)\right] \tag{A5}$$

Since

$$\lim_{a\to0}\frac{15}{16}(c_2+c_4)=1, \tag{A6}$$

$$\lim_{a\to0}\frac{15}{8}(-c_2+3c_4)=1, \tag{A7}$$

we have enhanced and decreased decay rates for the upper and lower sign, respectively.

(ii) Similarly, for $u=x,y$ the rate (A2) contains

$$2\gamma\left(\sum_{\alpha=1,2}\left[\frac{2}{5}|\tilde{\mathbf{d}}^{(\alpha)}|^2-\tfrac{1}{5}|\tilde{d}_u^{(\alpha)}|^2\right]+\frac{3}{32}(3c_0-2c_2-c_4)2\ \mathrm{Re}(\tilde{\mathbf{d}}^{(1)}\cdot\tilde{\mathbf{d}}^{(2)*})\right.$$
$$\left.-\frac{3}{32}(-c_0+6c_2-5c_4)2\ \mathrm{Re}(\tilde{d}_z^{(1)}\tilde{d}_z^{(2)*})\right)-\frac{3}{16}(c_0-2c_2+c_4)2\ \mathrm{Re}(\tilde{d}_u^{(1)}\tilde{d}_u^{(2)*})$$
$$=2\gamma\left[\frac{4}{5}\,|\tilde{\mathbf{d}}^{(1)}|^2\left(1\pm\frac{15}{64}(3c_0-2c_2-c_4)\right)-\frac{2}{5}|\tilde{d}_u^{(1)}|^2\left(1\pm\frac{15}{16}(c_0-2c_2+c_4)\right)\mp\frac{3}{16}|\tilde{d}_z^{(1)}|^2(-c_0+6c_2-5c_4)\right], \tag{A8}$$

which, by virtue of

$$\lim_{a\to0}\frac{15}{64}(3c_0-2c_2-c_4)=1, \tag{A9}$$

$$\lim_{a\to0}\frac{15}{16}(c_0-2c_2+c_4)=1, \tag{A10}$$

$$\lim_{a\to0}-c_0+6c_2-5c_4=0, \tag{A11}$$

gives rise to enhanced and decreased decay rates.

If $\Gamma_{\mathbf{m}\leftarrow\mathbf{n}}$ describes the creation or annihilation of a phonon in one of the modes of relative motion (i.e., $m_{ru}=n_{ru}\pm1$ for a certain $u\in\{x,y,z\}$) and the laser is tuned to resonance for some state $|\cdot,\pm1\rangle$, then $\tilde{\mathbf{d}}^{(2)}=\mp\tilde{\mathbf{d}}^{(1)}$ holds approximately. Hence, the above conclusions hold with the upper and lower sign exchanged: spontaneous emission from a state $|\cdot,-1\rangle$ is enhanced, and that from a state $|\cdot,+1\rangle$ is decreased.

APPENDIX B: INTERFERENCES

In this appendix, the interference of the amplitude **c** of the dipole-dipole–induced process with the amplitudes **b** and **d**

of the sideband cooling-heating and diffusion processes is investigated.

1. Interference of the $\mathbf{b}^{(\alpha)}$ and $\mathbf{c}^{(\alpha)}$ terms

It can be shown by using (49) and (14) or (A1) and (A2) that whether the j components of the $\mathbf{b}^{(\alpha)}$ and the $\mathbf{c}^{(\alpha)}$ interfere constructively or destructively depends on the relative phase of $b_j^{(1)}$ and $c_j^{(1)}$, i.e., the phase of $b_j^{(1)}c_j^{(1)*}$. In the following we investigate to what extent this phase can be chosen by adjusting the laser configuration.

The laser-field dependence of this phase is contained in

$$\left(\frac{\partial V_j}{\partial z}(\mathbf{X}^{(1)})-s\frac{\partial V_j}{\partial z}(\mathbf{X}^{(2)})\right)[V_j^*(\mathbf{X}^{(1)})+sV_j^*(\mathbf{X}^{(2)})] \quad \text{(B1)}$$

for $p=rz$, with the laser tuned to the upper or lower sideband resonance of state $|j,s\rangle$, and in

$$\left(\frac{\partial V_u}{\partial u}(\mathbf{X}^{(1)})-s\frac{\partial V_u}{\partial u}(\mathbf{X}^{(2)})\right)[V_z^*(\mathbf{X}^{(1)})+sV_z^*(\mathbf{X}^{(2)})] \quad \text{(B2)}$$

or

$$\left(\frac{\partial V_z}{\partial u}(\mathbf{X}^{(1)})-s\frac{\partial V_z}{\partial u}(\mathbf{X}^{(2)})\right)[V_u^*(\mathbf{X}^{(1)})+sV_u^*(\mathbf{X}^{(2)})] \quad \text{(B3)}$$

for $p=ru,u\in\{x,y\}$, with the laser tuned to the upper or lower sideband resonance of $|u,s\rangle$ or $|z,s\rangle$, respectively. In the following, (B1), (B2), and (B3) are discussed for $a\ll 1$.

(a) Case $p=rz$. For $s=-1$, (B1) becomes

$$\left(\frac{\partial V_j}{\partial z}(\mathbf{X}^{(1)})+\frac{\partial V_j}{\partial z}(\mathbf{X}^{(2)})\right)[V_j^*(\mathbf{X}^{(1)})-V_j^*(\mathbf{X}^{(2)})]. \quad \text{(B4)}$$

The last factor can be expressed as

$$V_j^*(\mathbf{X}^{(1)})-V_j^*(\mathbf{X}^{(2)})=r_0\left[\mathrm{Re}\left(\frac{\partial V_j}{\partial z}(z_{\mathrm{Re}}\hat{\mathbf{e}}_z)\right)+i\ \mathrm{Im}\left(\frac{\partial V_j}{\partial z}(z_{\mathrm{im}}\hat{\mathbf{e}}_z)\right)\right]^*, \quad \text{(B5)}$$

where the intermediate arguments $z_{\mathrm{Re}}\hat{\mathbf{e}}_z$, $z_{\mathrm{Im}}\hat{\mathbf{e}}_z$ lie between the equilibrium positions of the two ions: $z_{\mathrm{Re}},z_{\mathrm{Im}}\in(-r_0/2,r_0/2)$. By continuity of the derivative, (B4) has phase 0 in the limit $r_0\to 0$, provided that $(\partial V_j/\partial z)(0)\neq 0$. Therefore, apart from this last condition, for small equilibrium distances the relative phase in the interference term under consideration does not depend on the laser configuration.

In evaluating the phase of the other factors, it will be noted that for small a, the imaginary part in $f'(a)+\delta_{jz}g'(a)$ dominates and that $\nu_p\gg\gamma_{j,-1}$. Note that the sign of $\mathrm{Im}[f'(a)+\delta_{jz}g'(a)]$ is different for $j=x,y$, on the one hand, and $j=z$, on the other. For $j=x,y$, the result is destructive interference at the lower sideband and constructive interference at the upper sideband. This is illustrated in Fig. 7(a), with the laser chosen along the z axis and polarized in x direction: the peak in A_{rz-} at the lower sideband is smaller than the one in A_{rz+} at the upper sideband. Taking into account the matrix elements for the laser interaction, we see that the amplitude **c** has only about 6% of the size of the amplitude **b**, which results for the peaks in a ratio of $[(1+0.06)/(1-0.06)]^2\approx 1.27$. For $j=z$, the interference is constructive at the lower sideband and destructive at the upper one.

For $s=+1$, (B1) becomes

$$\left(\frac{\partial V_j}{\partial z}(\mathbf{X}^{(1)})-\frac{\partial V_j}{\partial z}(\mathbf{X}^{(2)})\right)[V_j^*(\mathbf{X}^{(1)})+V_j^*(\mathbf{X}^{(2)})]. \quad \text{(B6)}$$

The first factor can be expressed as

$$\frac{\partial V_j}{\partial z}(\mathbf{X}^{(1)})-\frac{\partial V_j}{\partial z}(\mathbf{X}^{(2)})=r_0\ \mathrm{Re}\left(\frac{\partial^2 V_j}{\partial z^2}(z_{\mathrm{re}}\hat{\mathbf{e}}_z)\right)+i\ \mathrm{Im}\left(\frac{\partial^2 V_j}{\partial z^2}(z_{\mathrm{im}}\hat{\mathbf{e}}_z)\right) \quad \text{(B7)}$$

which holds for some $z_{\mathrm{Re}},z_{\mathrm{Im}}\in(-r_0/2,r_0/2)$. In the limit of small distances, (B6) therefore has a phase of $\approx\pi$ if $\partial^2 V_j/\partial z^2(0)$ has the opposite phase of $V_j(0)$, as is the case for a *single* plane (running or standing) wave. In this case the same statement about destructive and constructive interferences at the upper or lower sideband holds as that found for $s=-1$, the phase of π in (B6) being compensated by the sign of the matrix element of H_{12}. But for more general laser fields, $\partial^2 V_j/\partial z^2(0)$ does not necessarily have the opposite phase of $V_j(0)$. Thus constructive interference at the lower sideband resonance for the state $|x,+1\rangle$, e.g., can be obtained by use of *two* traveling waves. Fig. 7(b) gives results for two traveling waves in the z and in the y directions, both polarized in the x direction and with appropriate phases so as to yield $V_x(\mathbf{x})\sim(e^{ikz}-2e^{iky})$, thus ensuring that $\partial^2 V_x/\partial z^2(0)$ has the same phase as $V_x(0)$. In agreement with the above discussion, the peak in A_{rz-} at the lower sideband resonance for state $|x,+1\rangle$ is clearly discernible in Fig. 7(b), while it was almost completely suppressed in Fig. 7(a). For the peak values of A_{rz+} at the upper sideband resonance for state $|x,+1\rangle$, it is the other way around, as predicted. Also in agreement with the prediction, the peak values at the lower and upper sideband resonances for state $|x,-1\rangle$ do not differ appreciably in Figs. 7(a) and 7(b).

(b) Case $p=rx,ry$. An analysis as above yields in the limit of small a that the laser-field dependence of the phase is determined by

$$\frac{\partial V_u}{\partial u}(0)\frac{\partial V_z^*}{\partial z}(0) \quad \text{(B8)}$$

[from (B2)] or

$$\frac{\partial V_z}{\partial u}(0)\frac{\partial V_u^*}{\partial z}(0) \quad \text{(B9)}$$

[from (B3)]. Here, even with only one traveling plane wave, different phases can be obtained by appropriately choosing

its direction and polarization. To show this, let $\mathbf{k}=(k_x,k_y,k_z)$ and $\boldsymbol{\epsilon}=(\epsilon_x,\epsilon_y,\epsilon_z)$ denote the directions of wave vector and polarization. Then the above phases are given by $k_u k_z \epsilon_u \epsilon_z^*$ and $k_u k_z \epsilon_u^* \epsilon_z$. Since $\mathbf{k}\cdot\boldsymbol{\epsilon}=0$, the general form of the polarization vector is $\boldsymbol{\epsilon}=w_1(-k_y,k_x,0)+w_2(-k_x k_z,-k_y k_z,k_x^2+k_y^2)$ and hence (choosing $u=x$)

$$k_x k_z \epsilon_x \epsilon_z^* = (k_x^2+k_y^2)(-w_1 w_2^* k_x k_y k_z - |w_2|^2 k_x^2 k_z^2),$$

$$k_x k_z \epsilon_x^* \epsilon_z = (k_x^2+k_y^2)(-w_1^* w_2 k_x k_y k_z - |w_2|^2 k_x^2 k_z^2),$$

and similarly for $u=y$. By adjusting the parameters k_x,k_y,k_z,w_1,w_2, these expressions can be given various phases; in particular they can be made positive or negative at will.

2. Interference of $\mathbf{b}^{(\alpha)}$ and $\mathbf{d}^{(\beta)}$ terms

Interferences between dipole-dipole interaction (amplitude **c**) and diffusion processes (amplitude **d**) occur whenever the laser is tuned to the central resonance for some intermediate state $|j,s\rangle$. The interference of **c** and **d** is less obvious than the one of **c** and **b** because **d** depends on the integration variable $\hat{\mathbf{k}}$, while **b** and **c** do not. Nevertheless, interference of **c** and **d** can be discussed by using the explicit formulas (A1) and (A2). The terms of interest here are the ones involving some $c_j^{(1)} d_j^{(1)*}$. (Note that we have $v_j^{(\alpha)} \approx c_j^{(\alpha)}$ at a central resonance and that (49) can be used to express $d_j^{(2)}$ in terms of $d_j^{(1)}$.) It is apparent in (A1) and (A2) that their importance is limited because of factors s_1 or s_3, which vanish in the limit $a \to 0$ [see (A3d) and (A3e). From (44b), (46), and (47) it follows that the laser direction(s) and polarization(s) enter via

$$|V_j(\mathbf{X}^{(1)}) + s V_j(\mathbf{X}^{(2)})|^2, \tag{B10}$$

the phase of which is always 0. The evaluation of the remaining factors at the central resonance for state $|j,s\rangle$ yields the following result in the limit of small a (cf. below).

For $p=rx,ry$ and any value of j, or for $p=rz$ and $j=z$, the interference is destructive in A_{p-} and constructive in A_{p+}. For $p=rz$ and $j=x,y$, the interference is constructive in A_{p-} and destructive in A_{p+}. In deriving these above statements it was assumed that in $f'(a)$, $f'(a)+g'(a)$, and $g(a)$, the imaginary parts are bigger in modulus than the real parts, which holds for small a.

3. Interference far from any resonance

The previous discussion focused on the effect of interferences at some resonance. If the laser is detuned between the resonances, the cooling and heating coefficients decrease by orders of magnitude. The theoretical analysis becomes more complicated because contributions involving different states may then be equally important. Nevertheless we would like to mention a qualitative difference in comparison with the single atom case: there, for any negative laser detuning, the cooling coefficient A_- is bigger than the heating coefficient A_+, and the reverse holds for any positive detuning. This is no longer true in the two-ion case, as becomes apparent when Fig. 7(a) is replotted by using a logarithmic scale; see Fig. 8(a). The occurrence of $A_{r3-} < A_{r3+}$ (heating) for certain negative detunings and of $A_{r3+} < A_{r3-}$ (cooling) for some positive ones can be traced to the interference term

$$(\tfrac{1}{2}s_1 + \tfrac{1}{2}s_3)\mathrm{Re}(\mathbf{v}^{(1)}\cdot\mathbf{d}^{(2)*} - \mathbf{v}^{(2)}\cdot\mathbf{d}^{(1)*}) \tag{B11}$$

in (A1). In Fig. 8(b) the resulting average phonon number $\langle n_{rz}\rangle$ is plotted. It summarizes the effects discussed above: the existence of two local minima at the lower sideband reflects the splitting of the resonance by the dipole-dipole interaction. There is a region where cooling is possible (to a certain extent) with a close to zero or even a blue laser detuning, and, as predicted, there is an interval where no cooling is possible in spite of a red laser detuning.

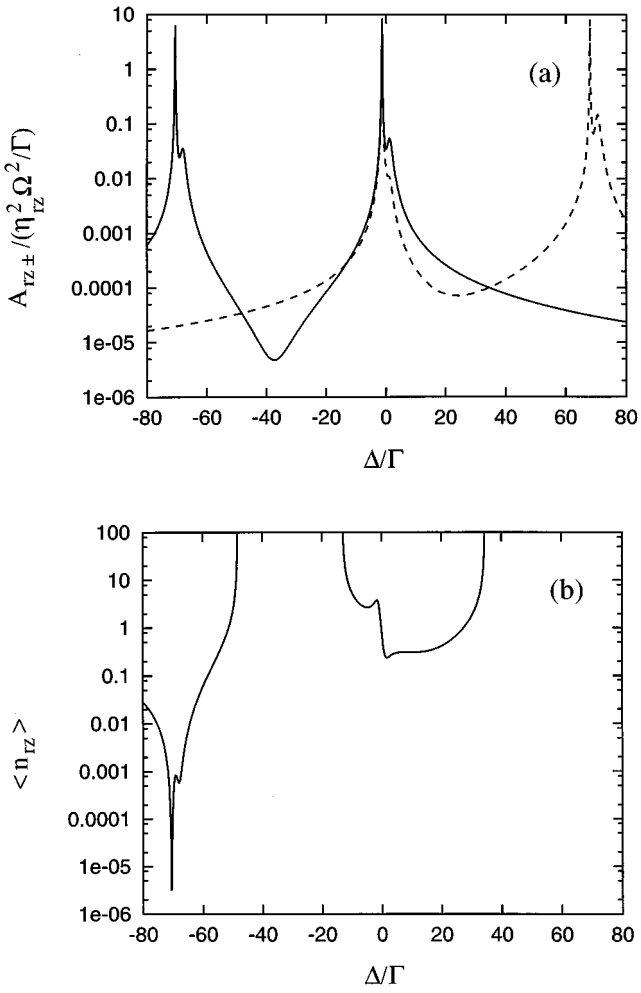

FIG. 8. (a) Same as Fig. 7(a), using a logarithmic scale. (b) Average phonon numbers resulting in steady-state regime from A_{rz-} (solid curve) and A_{rz+} (dashed curve) in (a). $\Gamma \equiv 2\gamma$.

[1] J. M. Doyle, J. C. Sandberg, I. A. Yu, C. L. Cesar, D. Kleppner, and T. J. Greytak, Phys. Rev. Lett. **67**, 603 (1991); C. R. Monroe, E. A. Cornell, C. A. Sackett, C. J. Myatt, and C. E. Wieman, *ibid.* **70**, 414 (1993); W. Ketterle, K. B. Davis, M. A. Joffe, A. Martin, and D. E. Pritchard, *ibid.* **70**, 2253 (1993); I. D. Setija, H. G. C. Werij, O. J. Luiten, M. W. Reynolds, T. W. Hijmans, and J. T. M. Walraven, *ibid.* **70**, 2257 (1993); R. J. C. Spreeuw, C. Gerz, L. S. Goldner, W. D. Phillips, S. L. Rolston, C. I. Westbrook, M. W. Reynolds, and I. F. Silvera, *ibid.* **72**, 3162 (1994).
[2] F. Diedrich *et al.*, Phys. Rev. Lett. **59**, 2931 (1987).
[3] D. J. Wineland *et al.*, Phys. Rev. Lett. **59**, 2935 (1987).
[4] M. G. Raizen, *et al.*, Phys. Rev. A **45**, 6493 (1992).
[5] H. Walther, Adv. At. Mol. Opt. Phys. **32**, 379 (1994).
[6] R. Blatt, in *Atomic Physics 14*, edited by D. Wineland, C. Wieman, and S. Smith (AIP, New York, 1995), p. 219.
[7] See, for example, *The Physics of Trapped Ions*, edited by R. Blatt, P. Gill, and R. C. Thompson, special issue of J. Mod. Opt. **39**, 192 (1992).
[8] J. Guo (unpublished).
[9] R. G. Brewer, R. G. DeVoe, and R. Kallenbach, Phys. Rev. A **46**, 6781 (1992).
[10] C. Monroe *et al.* (unpublished).
[11] R. G. DeVoe (unpublished).
[12] R.H. Dicke, Phys. Rev. A **93**, 99 (1954).
[13] L. Gilbert and C. E. Wieman, Opt. Phonics News **4**, 8 (1993).
[14] J. Dalibard, Opt. Commun. **68**, 203 (1988).
[15] D. W. Sesko, T. G. Walker, and C. E. Wieman, J. Opt. Soc. Am. **8**, 946 (1991).
[16] A.M. Smith and K. Burnett, J. Opt. Soc. Am. B **8**, 1256 (1991); **9**, 1256 (1991); A. M. Smith, K. Burnett, and P. Julienne, Phys. Rev. A **46**, 4091 (1992); G. Hillenbrand, C. Foot, and K. Burnett, *ibid.* **50**, 1479 (1994); M. Holland, K.-A. Suominen, and K. Burnett, *ibid.* **50**, 1513 (1994); Phys. Rev. Lett. **72**, 2367 (1994); K. Ellinger, J. Cooper, and P. Zoller, Phys. Rev. A **49**, 3909 (1994).
[17] See, for example, S. Stenholm, Rev. Mod. Phys. **58**, 699 (1986), and references therein.
[18] J. Javanainen, J. Opt. Soc. Am. B **5**, 73 (1988).
[19] J. M. Raimond, P. Goy, M. Gross, C. Fabre, and S. Haroche, Phys. Rev. Lett. **49**, 117 (1982); **49**, 1924 (1983).
[20] M. Gross and S. Haroche, Phys. Rep. **93**, 301 (1982), and references therein.
[21] D. J. Wineland, W. M. Itano, J. C. Bergquist, and R. G. Hulet, Phys. Rev. A **36**, 2220 (1987).
[22] J. I. Cirac, R. Blatt, P. Zoller, and W. D. Phillips, Phys. Rev. A **46**, 2668 (1992).
[23] R. H. Lehmberg, Phys. Rev. A **2**, 883 (1970); **2**, 889 (1970).
[24] We wish to emphasize that for $\zeta_u > 1$, quantum statistical effects should be taken into account. However, this requires exceedingly high trap frequencies so that among other things a relativistic analysis would be required.
[25] J. I. Cirac, L. J. Garay, R. Blatt, A. S. Parkins, and P. Zoller, Phys. Rev. A **49**, 421 (1994).